IN VITRO STUDY OF SYNTHETIC PROSTHETIC MESHES FOR INGUINAL HERNIA REPAIR

by

JING CAO

(Under the Direction of Suraj Sharma)

ABSTRACT

Inguinal hernia is a protrusion of part of viscera through the abdominal wall. The prosthetic mesh is widely used in inguinal hernia repair, where it is implanted in place to make up the hernia defects and further repair is enhanced by host tissue ingrowth into the mesh. Due to the significance of the implant for successful hernia repair, there is increasing need for understanding the roles of mesh materials and constructions in order to design ideal prosthetic mesh. This study used an in *vitro* model by growing NRK-49F cells on synthetic prosthetic meshes, which differed in types of materials (polypropylene (PP), polyester (PET), polytetrafluoroethylene (PTFE)) and weights (lightweight, heavyweight), to compare the difference in biological and mechanical responses of these meshes after implantation.

Cell morphology and cell proliferation on the meshes were investigated to predict the biological response in the recipient. PP and PET meshes induced acute initial foreign body reaction, implying better cell/tissue incorporation than PTFE mesh. Weight reduction could weaken the foreign body reaction, leading to well organized cellular layer wrapping the prosthetic materials. The mechanical response was studied by performing of tensile testing and

dynamic mechanical simulation on the vital/avital composite meshes. The results demonstrated that cell incorporation significantly increased the stiffness of heavyweight PP and PET meshes; however, lightweight PP mesh could inhibit this increase and reduce the complication of ‘stiff abdomen’ in the long-term. Additionally, the cell incorporation also contributed to mechanical reinforcement of the meshes after implantation and it could ensure the mechanical integrity of the implants in the long-term.

INDEX WORDS: Prosthetic hernia mesh, *In vitro*, Vital/avital composite mesh, Cell incorporation, Stiffness

IN VITRO STUDY OF SYNTHETIC PROSTHETIC MESHES FOR INGUINAL HENRIA REPAIR

by

JING CAO

B.S., Beijing Institute of Clothing and Technology, China, 2008

A Thesis Submitted to the Graduate Faculty of The University of Georgia in Partial Fulfillment of the Requirements for the Degree

MASTER OF SCIENCE

ATHENS, GEORGIA

2010

IN VITRO STUDY OF SYNTHETIC PROSTHETIC MESHES FOR INGUINAL HERNIA REPAIR

by

JING CAO

Major Professor:	Suraj Sharma
Committee:	Ian R. Hardin
	Patricia A. Annis

Electronic Version Approved:

Maureen Grasso
Dean of the Graduate School
The University of Georgia
August 2010

DEDICATION

This thesis is dedicated to my dear grandfather and my dear parents, for their forever love and support.

ACKNOWLEDGEMENTS

This thesis would never have been completed without help and support of people who are gratefully acknowledged here.

Foremost, sincere thanks to my major advisor, Dr. Suraj Sharma, for his great insight in the proposal of the research and his substantial assistance and guidance throughout my entire course of study and research at the University of Georgia.

Special thanks to my committee members, Dr. Ian R. Hardin and Dr. Patricia A. Annis, for their valuable suggestions, ideas and comments in the research.

I am very grateful to the faculty, staff, and graduate students from the Department of Textiles, Merchandising and Interiors for their cooperation and help.

I would like to extend my thanks to Dr. Arthur Gride from Department of Food and Nutrition for instrumentation support, and PhD student Yongjun Wen from College of Veterinary Medicine for technical help.

My deep appreciation goes to my lovely families for their endless love, support and confidence on me.

TABLE OF CONTENTS

Page

ACKNOWLEDGEMENTS v

LIST OF TABLES viii

LIST OF FIGURES ix

CHAPTER

1 Introduction 1

1.1 Statement of Problem 2

1.2 Objective of Study 3

2 Literature Review 4

2.1 Biology of Inguinal Hernia Formation 4

2.2 Techniques of Inguinal Hernia Repair 5

2.3 Biological Response of Prosthetic Mesh 7

2.4 Category of Prosthetic Mesh 10

2.5 Mechanical Property of Prosthetic Mesh 13

2.6 Summary of Literature Review 15

3 Materials and Methods 17

3.1 Prosthetic Hernia Meshes 17

3.2 Cell Culture 18

3.3 Formation of Vital/avital Composite Mesh 18

3.4 Biocompatibility of Prosthetic Hernia Mesh 19

3.5 Mechanical Response of Prosthetic Hernia Mesh 20

4 Results and Discussions 24

4.1 Major Properties of Prosthetic Hernia Mesh 24

4.2 Cell Incorporation of Prosthetic Hernia Mesh 25

4.3 Initial Foreign Body Reaction of Prosthetic Hernia Mesh 30

4.4 Mechanical Property of Vital/avital composite mesh 33

5 Conclusions and Future Work 41

5.1 Conclusions 41

5.2 Future Work 42

REFERENCES 43

APPENDICES 52

LIST OF TABLES

Pages

Table 2.1: Categories of mesh weight, pore size and filament structure 11

Table 2.2: Examples of biological mesh.....11

Table 3.1: Properties of sample prosthetic meshes.....17

LIST OF FIGURES

Pages

Figure 2.1: Schematic of the biological response to a synthetic prosthetic 8

Figure 3.1: Schematic of mechanical simulation 21

Figure 4.1: SEM of heavyweight vital/avital composite meshes 27

Figure 4.2: SEM of lightweight vital/avital composite meshes 29

Figure 4.3: Optical density of formazan solution to determine proliferation of NRK-49F cells after contacting with different prosthetic meshes..... 31

Figure 4.4: Tensile stress-strain diagram of PP601 mesh and its vital/avital composite mesh 34

Figure 4.5: Elastic modulus of vital/avital composite mesh compared with its control (without cells).....35

Figure 4.6: Ultimate strength of vital/avital composite mesh compared with its control (without cells).....36

Figure 4.7: Storage modulus of vital/avital composite mesh during dynamic mechanical simulation.....37

Figure 4.8: Percent change of storage modulus of mesh and it vital/avital composite during dynamic mechanical simulation.....39

CHAPTER 1

INTRODUCTION

Inguinal hernia, named for its anatomical location, is a protrusion of the part of viscera through the abdominal wall when it does not effectively provide the mechanical strength and flexibility necessary to counteract the pressure force exerted by the viscera within abdominal cavity. Inguinal hernia is one of the most common afflictions for adults, and the lifetime risk to develop inguinal hernia is 27% for men and 3% for women [1]. This gender difference is probably because of the polygenetic trait involving hernia formation. Approximately 770,000 operations of inguinal hernia repair are performed each year in the United States [2].

The hernia repair has evolved through advances in anatomical and repair techniques, similar to other surgical procedures. A true leap forward in operative technique of hernia repair was the invention of a tension-free repair, where a prosthetic mesh is imported in place to approximately make up the hernia defects, and further repair is enhanced by scar tissue ingrowth into the mesh. In the view of clinical data, adopting mesh for hernia repair significantly reduced the rate of recurrence that was regarded as the primary complication associated with hernia repair [3]. The ideal hernia mesh should be nontoxic and sufficiently biocompatible to support tissue ingrowth and should not provoke an acute inflammatory response in the host. Furthermore, and perhaps most importantly, it should not be modified by excretive chemicals during foreign body reaction and be resistant to mechanical strains. Typically, synthetic (absorbable and nonabsorbable) prosthetic meshes and biologic grafts are used for inguinal hernia repair.

Although the best mesh material for hernia repair is still unknown, the potential benefits of synthetic mesh have been explored and studied mostly because of its abundant supply, low cost and easy modification and production.

1.1 Statement of Problem

In clinical practice, the alloplastic biomaterials, namely polypropylene (PP), polyester (PET) and polytetrafluoroethylene (PTFE), are widely used to reinforce the ruptured abdominal wall. The mechanical properties of these implants are critical for the success of hernia repair and are mainly regulated by the initial foreign body reaction and local tissue incorporation of prosthetic meshes after implantation in the recipient [4-5]. Although surgical hernia meshes have been confirmed to be not associated with an increased risk of malignant tissue degeneration [6-7], some implant-determined postoperative problems remain unsolved, such as mesh shrinkage, foreign body sensation and the phenomenon of “stiff abdomen”, which are affected by material and constructional characteristics of implanted prosthetic meshes [8-10]. Previous research has done little to compare the initial biological responses to different mesh materials after implantation. The comparison of extents of foreign body reaction caused by PP, PET and PTFE meshes has not yet reached agreement [11-12]. Regarding mesh constructions, the weight of an implanted mesh has become the most discussed parameter. Newly developed meshes have decreased weight to reduce the foreign body response, a result that has been supported by some animal studies [9, 13]. However, several studies have argued the leading role of material amount and stressed other parameters such as pore size and fibrous structure might be of importance for biological response to implanted meshes [14-16]. Therefore, there is a need to investigate

properties and lifetime of prosthetic mesh after implantation for understanding the roles of mesh materials and its constructions in order to design the ideal prosthetic mesh for hernia repair.

1.2 Objective of Study

The main objective of this study was to use an *in vitro* model by growing cells on prosthetic hernia meshes that differed in type of materials and weights, to investigate the influence of these parameters on biological response and mechanical response of the meshes after implantation.

There were several specific objectives of this research, as listed below:

1) Determine proper cell culture to create vital/avital composite meshes.
2) Investigate the influence of mesh materials (PP, PET, PTFE) on biocompatibility of hernia mesh in *in vitro* study. The property of biocompatibility includes cell morphology and cell proliferation on hernia meshes.
3) Investigate the influence of mesh weights (heavyweight and lightweight) on biocompatibility of PP hernia mesh in *in vitro* study.
4) Study the time-independent mechanical properties of vital/avital composite meshes, including the change in elastic modulus and ultimate strength.
5) Establish the mechanical simulation model to study the time-dependent mechanical properties of vital/avital composite meshes.

CHAPTER 2

LITERATURE REVIEW

For a thorough understanding of this research study, the following five fundamental components are included in this literature review: 1) biology of inguinal hernia formation, 2) techniques of inguinal hernia repair, 3) biological response to prosthetic mesh, 4) category of prosthetic mesh, 5) mechanical property of prosthetic mesh.

2.1 Biology of Inguinal Hernia Formation

Since Fruchaud began the discussion of hernia anatomy in 1956, numerous studies focusing on hernia as a disease of extracellular matrix (ECM) put forward the unified theory of hernia formation that disturbances in collagen metabolism contribute to direct inguinal and incisional hernias [17]. The collagens are major constituents of the ECM, and they are in a dynamic balance of synthesis and degradation by matrix metalloproteinases (MMPs). The MMP family includes at least 23 gene products, which belong to a larger category of proteases known as the metzincin superfamily. Studies showing that MMP-2 [18] and MMP-13 [19] over-expression were measured in patients with both direct and recurrent inguinal hernias. Another study demonstrated that the decrease in ratio of type I collagen and type III collagen was responsible for hernia formation because it played an important role in the solidity of the collagen strand and the determination of the final fibril diameter and bundle architecture [20]. There are 29 types of collagens identified in the body, making up about 25% to 35% of the

whole-body protein content. Type I collagen, forming a network of thick fiber bundles, predominantly provides tensile strength, whereas type III collagen consists of nonpolymeric thinner fibers and is regarded as a temporary matrix during tissue remodeling. Therefore, a shift of the collagen ratio in favor of type III collagen compromises the mechanical function of abdominal wall, resulting in inguinal hernia.

Morphologic and molecular investigations in hernia patients underscore the significance of impaired wound-healing after repair operation. One mechanism for wound-healing failure is the loss of force signaling from the abdominal wall that induces the defects in regenerative tissues. This is because mechanical forces are required to stimulate the cell growth and hence the repair of tissues and tendons [21]. Alternations in MMP-2 and corresponding fibrillar collagen expression also interfere with the wound-healing process. Furthermore, family histories from hernia patients indicated an increased familial incidence of hernia, raising the premise that genetic traits might predispose to hernia formation [17].

2.2 Techniques of Inguinal Hernia Repair

The repair of inguinal hernia represents the most frequent operations performed by general surgeons. The probability of the successful repair has increased as a result of the improvement in surgical equipments and the innovation of repair techniques.

2.2.1 Tissue-based repair

In 1887, Bassini invented tissue-based repair technique, which was considered as the beginning of contemporary inguinal hernia surgery. The operation was performed through a 7- to 10-cm incision along the inguinal ligament, and then the silk sutures were placed with a metal stitch to incorporate the lateral margin of the abdominal muscle. This repair technique resulted in

large force on silk sutures, causing their mechanical failure. That would lead to the recurrence of hernia. Therefore, on the basis of Bassini repair, many innovations of the tissue-based repair emerged in an attempt to decrease the high rate of recurrence due to the high tension at suture site. For example, the McVay repair employed a relaxing incision technique to reduce the tension and is still performed currently for femoral hernias [22]. Another outstanding modification was the Shouldic repair, in which the silk suture was replaced by the stainless steel suture. This repair quickly became the gold standard for open hernia repair until the prosthetic mesh repair had been universally adopted in the 1980s.

2.2.2 Prosthetic mesh repair

In 1984, Lichtenstein invented another hernia repair technique and this method kept repair tension at an absolute minimum with a piece of an implanted mesh [23]. The Lichtenstein repair, dubbed ‘tension-free repair’, has been showing significantly less recurrence rates when compared with the tissue-based hernia repair. According to the literature data, recurrence rates after the tissue-based repair of inguinal hernia vary between 4.4 and 17% [24-25], while recurrence rates for mesh repair vary between 0.3 and 2.2% [24]. The family of prosthetic mesh repairs can be categorized by the anatomic location, such as Lichtenstein repair (anterior position), Kugel repair (prepertioneal position), Plug repair (cone-shaped) and Stoppa repair (bilateral structure). Although tension-free mesh repairs have brought about significant improvements in surgical and clinical reported outcomes, the foreign body reaction to the implanted prosthetic materials and their mechanical stabilities in the long-term implantation complicated the application of mesh repair for inguinal hernia.

2.3 Biological Response of Prosthetic Mesh

The ideal prosthetic mesh should minimize the foreign body response, adequately incorporate within host tissue and resist the degradation by all kinds of excretive chemicals in the recipient, all of which are significantly influenced by the biological response to the mesh after implantation.

2.3.1 Short-term biological response

After prosthetic mesh is implanted, an extraordinary complex series of reaction takes place in the recipient (*Figure 2.1*). Immediately after implantation, the mesh adsorbs host proteins that create a coagulum layer around it. This process only takes few seconds to isolate the foreign body from the host body. Platelets adhere to the protein coagulum and release a host of chemoattractants that induce more platelets, polymorphonucleocytes (PMNs), macrophages, fibroblasts and smooth muscle cells to the implant site. The PMNs continuously release proteases to destroy the implanted mesh and further attract macrophages, fibroblasts and smooth muscle cells. Macrophages populate the implanted site to consume the foreign bodies, dead organisms and tissue, and ultimately coalesce to form the foreign body giant cells at tissue/material interfaces. The foreign body giant cells, which stay in the area for indefinite time, incessantly release mediators of degradation such as reactive oxygen intermediates (ROIs), degradative enzymes and acids into tissue/material interfaces to destroy the implant [26]. Additionally, the fibroblasts and smooth muscle cells systematically secrete monomeric fibers that would polymerize into the helical structure of collagen, deposited in the ECM. The regenerative collagen would have a loss in proportion of type I (mature) to type III (immature) collagens. The type I collagen consists of helical polymer chains that determines the overall strength and elasticity of regenerative tissues. Hence, the decrease in type I collagen leads to a relatively less

elastic tissue, which has only 70 to 80% strength of the native connective tissue [27]. It is for this reason that the mechanical integrity of a prosthetic mesh is important for the long-term success of hernia repair. Furthermore, the scar and connective tissues surrounding the prosthetic mesh would cause its contraction in dimension, thus reducing the area originally covered by the implanted mesh that would cause the recurrence of hernia.

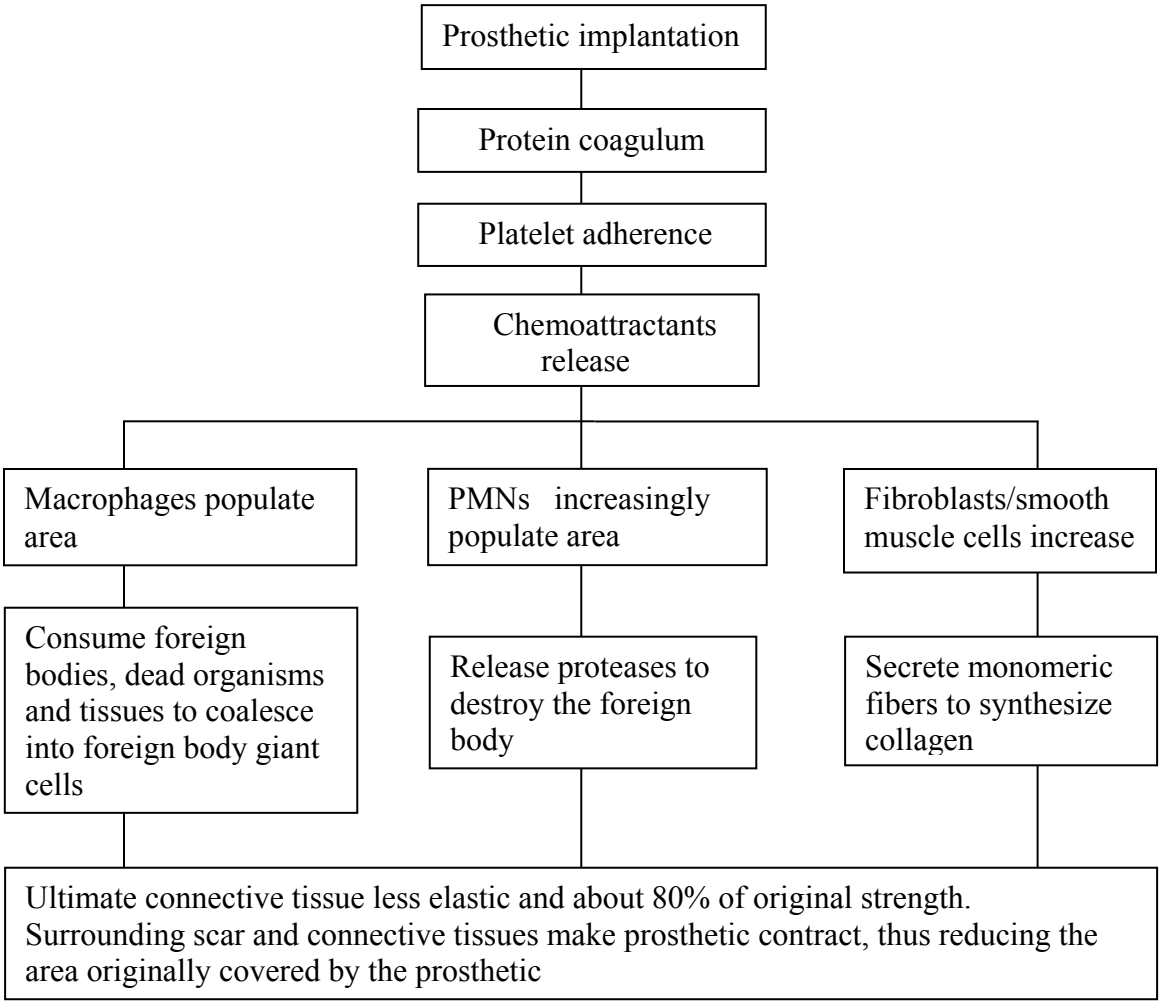

Figure 2.1 Schematic of the biological response to a synthetic prosthetic. Note: PMNs, polymorphonucleocytes

2.3.2 Long-term biologic response

The knowledge of biologic response to mesh after long-term implantation is not fully understood, though some data from animal studies and meshes explanted from patients, suggested following serious complications associated with long-term implantation of prosthetic hernia meshes:

Recurrence after mesh implantation appears in 26 months on average, with a range from 3 to 180 months. Approximately 60% of the mesh repair failures was caused by the recurrence, despite the fact that the recurrence rate of hernia mesh repair has significantly decreased compared to the tissue-based repair [28]. The main reasons for recurrence are the loss of initial load bearing, the shrinkage of the prosthetic mesh and the alternation of the extracellular matrix.

Chronic Pain is an upcoming issue in patient reports after prosthetic mesh repair. The incident of chronic pain after inguinal hernia repair varies from 9.7 to 51.6% in different studies [29-31]. The chronic pain is typically lasts for one year after implantation. Several studies demonstrated the presence of nerve fibres and fascicles (a bundle of nerve fibers enclosed by the perineurium) at the surface of most explanted meshes that were removed due to chronic pain. These findings raise the speculation that the nature of the foreign body giant cells causes the sensation of chronic pain [28]. It was because small nerve structures were found in the foreign body giant cells, according to the study of immunohistochmeical strains.

Infection is the third major complication after mesh implantation. The clinical studies showed that the rate of postoperative infection associated with hernia mesh repair was similar for all currently used mesh materials, but different for the materials with different physical structures [32].

Stiff Abdomen, which refers to reduced compliance of the abdominal wall, is the most serious complication after hernia mesh repair. All hernia meshes after implantation inevitably caused an increased stiffness of the abdominal wall to some degree, which was well demonstrated by ultrasound examination and 3D stereography in patients having mesh repair [9, 33], though the extents of stiffness increase were significantly affected by mesh materials, weights and pore size. The formation of stiff abdomen involves essentially all chemical components in the inflammatory response, and is a physiological process of reconstruction of normal tissue surface.

2.4 Category of Prosthetic Mesh

The prosthetic meshes for hernia repair can be categorized according to the constructional parameters such as weight and pore size as shown in *Table 2.1,* or on the basis of the raw materials as described below:

2.4.1 Biological mesh

Biological mesh materials are based on collagen scaffolds derived from a donor, which can be attributed to different donor sources, such as xenografts (from other species), allografts (from other individual of the same species) and autografts (from same individual). *Table 2.2* shows different kinds of biological meshes. The advantage of the biologic mesh is less susceptibility to cause foreign body response, but their mechanical stabilities in *in vivo* require improvement before wide spread use as a primary mesh for inguinal hernia. There was some early research on the use of biological mesh for inguinal hernia repair, such as xenogeneic mesh made from porcine small intestinal submucosa [34]. However, there are no current published clinical reports on the use of pure biological mesh for hernia repair in humans.

Table 2.1 Categories of mesh weight, pore size and filament structure [35]

Parameters	Categories
Weight	Heavyweight: > 90 g/m^2 Mediumweight: 50 – 90 g/m^2 Lightweight: 35 – 50 g/m^2 Ultra-lightweight: < 35 g/m^2
Pore size	Very large pore: > 2000 μm Large pore: 1000 – 2000 μm Medium pore: 600 –1000 μm Small pore: 100 – 600 μm Microporous: < 100 μm
Filament	Monofilament Doubled filament Multifilament

Table 2.2 Examples of biological mesh [36]

Category	Brand name (company; price)
Human dermis	AlloDerm (LifeCell; \$26.08/cm^2) AlloMax (Bard/Davol; \$26.00/cm^2) FlexHD (MTF)
Porcine dermis	Permoacol (TSL; \$8.33/cm^2) Collamend (Bard/Davol; \$16.00/cm^2) Strattice (LifeCell) XenMatrix (Brennan Medical)
Porcine small intestine submucosa	Surgisis (Cook; \$3.40/cm^2)
Fetal bovine dermis	SurgiMend (TEI Bioscience; \$22.00/cm^2)

2.4.2 Nonabsorbable synthetic mesh

Polypropylene (PP), polyester (PET) and polytetraflouroethylene (PTFE) are the most common raw materials for nonabsorbable synthetic hernia mesh. Many *in vitro* or *in vivo* studies have been conducted to investigate their biologic response and the clinical results. The results showed that these meshes induced different biological response depending on its materials and fibrous structures. PP mesh (e.g., Prolene®, Marlex®, Surgipro®) is hydrophobic and susceptible to oxidation, whereas PET mesh (e.g., Dacron® Mersilene®) is resistant to oxidation but has propensity to hydrolysis. Gonzales et al. showed that both PP and PET meshes exhibited adequate biocompatibility to integrate into the host tissue; the mesh incorporation of the tissue is proportional to its pore size and amount of materials [37]. However, both meshes led to high adhesion with viscera, which limited their use in some anatomic locations. PTFE mesh was used for the first time in hernia surgery in 1959, but it caused high recurrence rates due to low tensile strength and lack of incorporation within tissue [38]. Currently available hernia mesh made of PTFE polymer is expanded PTFE mesh (ePTFE, Gore-Tex®) that has microscopic pores. The primary advantage of ePTFE mesh is that it has lower incidence of visceral adhesion than PP and PET meshes [39].

2.4.3 Composite mesh

The composite mesh, different from vital/avital composite mesh, refers to the kind of mesh made by two or more different biomaterials. Currently, two kinds of composite meshes are used for hernia repair. One is having two layers in which each layer is made of different materials. Another is produced by combining nonabsorbale polymer and absorbable polymer in one-layer. The ideal two-layer composite mesh would have opposite functions in each side: the surface exposed to the viscera would resist adhesion, whereas other side would encourage mesh

ingrowth into the tissue. PP/ePTEF composite mesh (Gore Dualmesh®) is the two-layer composite mesh, where the PP side facing to abdominal wall supports tissue ingrowth while the ePTEF side repels ingrowth with the visceral surface. However, some serious problems from two-layer composite mesh occur when there is a differential in contraction between two layers, which leads to the rolling of mesh edges to the opposite side [40]. Vypro II® mesh is a one-layer composite mesh which is composed of nonabsorbable PP mesh and absorbable polyglactin to reduce the density of the mesh, yet maintaining enough mechanical strength [35]. Another available one-layer composite mesh has a temporary component of absorbable materials that provides a barrier between the mesh and the viscera, such as collagen-coated PET mesh or oxidized-regenerated-cellulose-coated PP mesh. This is due to the better biocompatibilities of these absorbable materials, and thus induce less foreign body reaction than pure nonabsorbable meshes.

2.5 Mechanical Property of Prosthetic Mesh

The mechanical properties of implanted meshes is significant in determining the success of inguinal hernia repair. These meshes should not only reconstruct the abdominal wall, but also have sufficient fatigue strength to ensure their long life *in vivo*. It was clinically found that complications of prosthetic meshes are often associated with mechanical and structural incompatibility between the implants and host tissues, and the change of their mechanical properties during implantation *in vivo* [41]. Ingrowing cells and extracellular matrix deposition transform the mesh fibers into bundles with higher bending stiffness. Meanwhile, the friction between fibers also increases. Both effects can considerably increase the mesh stiffness [42]. Klinge and Klosterhalfen demonstrated in animal models [43-44] and explanted meshes [45]

after clinical excisions that polypropylene mesh significantly decreased the mobility of the abdominal wall after 2 – 3 weeks' implantation, which was caused by the induction of strong and unorganized scar formation around the fibers. Moreover, Schumpelick argued that mechanical properties of commonly used meshes exceeded the abdominal wall several time in terms of bending resistance and stiffness [46]. Usually, the prosthetic mesh, after implantation, induces host cells around it and creates a vital/avital composite material. If the stiffness of this composite greatly exceeds that of the ingrown tissue, most of the mechanical loading will be borne by the implant, and the load-deprived host tissues will lack the mechanical simulation to induce their regeneration and maturation. Thus, it is imperative to properly understand the mechanical behaviors of those vital/avital composites for designing an ideal prosthetic hernia mesh. In tissue engineering, one of the effective approaches is the use of an *in vitro* model by growing isolated cells on prosthetic mesh to construct the vital/avital composite, and then further investigation of their mechanical properties. Time-independent and time-dependent testing protocols are commonly used methods to identify and predict the mechanical properties of biomaterials in their application [47].

2.5.1 Time-independent behavior

Tensile or compressive loading is the most common method for mechanical testing and is used to determine several material characteristics such as linear or nonlinear behavior, fatigue strength and fracture limit. During testing, increasing levels of tensile or compressive forces are slowly applied to the test specimen, and instruments such as extensometers are used to precisely measure the strain from the change in length of two points within the testing section (*Equation 2.1*):

$$\epsilon = (L' - L_0)/L_0 \quad (2.1)$$

where ϵ is the strain, L' the final length of sample, L_0 the original length of the sample.

If large strains ($\epsilon > .05$) are observed before fracture, it is common to calculate the true strain (ϵ'):

$$\epsilon' = \ln(1 + \epsilon) = \ln(L'/L_0) \quad (2.2)$$

Ultimate strength σ' is determined from the force required to cause failure F' and the original cross sectional area A_0

$$\sigma' = F'/A_0 \quad (2.3)$$

2.5.1 Time-dependent behavior

Because most biological tissues exhibit viscoelastic behavior, it is important to investigate viscoelastic properties of biomaterials by time-dependent dynamic mechanical testing. Creep and relaxation are the most common types of viscoelastic testing, where a known stress or strain applied to the materials and corresponding strain or stress is monitored over time. In a few *in vitro* culture studies, the dynamical mechanical simulation was conducted to the vital/avital composites to investigate the cell response under forced simulation and predict the composites' mechanical biocompatibility with host tissues [41, 48].

2.6 Summary of Literature Review

The introduction of prosthetic mesh to support hernia repairs has achieved satisfactory results with the overall recurrence rate of less than 10% [49], but the best mesh material and its structural design for hernia repairs is yet unknown. Reducing the negative consequences of the inflammatory reaction, yet maintaining the mechanical stabilities of implanted meshes, is the

subject of current research. The optimal way to accomplish this goal is unclear; current strategies include reducing the mesh weight, changing its physical structure and blending the nonabsorbable mesh with the absorbable components.

The prosthetic mesh, after implantation, induces host cells around it and creates a vital/avital composite material. This composite mesh exerts a significant role in hernia repair, such as providing enough mechanical force or supporting tissue regeneration. The reasons for the failure of the composite generally include acute inflammatory response, unsatisfying integration with tissue ingrowth, and unstable mechanical properties. Many studies on biologic response to the vital/avital composite have been conducted in both *in vitro* and *in vivo* studies; however, studies on its mechanical properties are sparse. The mechanical stability of prosthetic mesh is important for the long-term success of hernia repair due to 20 to 30% elastic loss of regeneration tissue after hernia repair. Thus, the lack of knowledge about properties of vital/avital composites is one of the major obstacles to achieve ideal clinical outcomes of inguinal hernia repair.

In addition, it is well known that *in vitro* culturing techniques are useful for determination of foreign body reaction [14-15], investigation of material biocompatibility [50], and construction of vital/avital composites [41]. The use of a cell culture *in vitro* study has potential to create a single cell model in accordance with the specific environment, which avoids interference from extracellular influence on cell response. For this reason, the one-dimensional *in vitro* models are required as first-line experimental design for biomaterial research before conducting *in vivo* studies.

CHAPTER 3

MATERIALS AND METHODS

3.1 Prosthetic Hernia Mesh

Three polypropylene (PP) hernia meshes, one polyester (PET) hernia mesh and one polytetrafluoroethylene (PTFE) hernia mesh (Textile Department Associates, Inc., New York) were chosen to investigate the influence of material and constructional parameters on biocompatibilities and mechanical properties of hernia meshes. Major physical and mechanical properties of these meshes were summarized in *Table 3.1*.

Table 3.1 Properties of sample prosthetic meshes

Prosthetic mesh		**PP403**	**PP404**	**PP601**	**PET**	**PTFE**
Type		doubled filament	mono filament	doubled filament	multi filament	doubled filament
Weight, g/m^2		45	41	100	125	98
Thickness, mm		0.43	0.36	0.61	0.53	0.38
Filament diameter, μm		100	100	150	20	150
Mean pore size, μm		1150	580	1150	1050	1500
Porosity, %		58	55	47	48	48
Burst strength, N		585	510	1063	758	518
Break strength (N/2.5 cm)	**MD**	228	129	512	384	307
	CMD	220	182	489	395	316
Elastic modulus, MPa		6.15	4.03	11.89	9.66	3.67

3.2 Cell Culture

Cell cultures are useful for the investigation of materials' biocompatibility [51]. The cell line, consisting of fibroblasts NRK-49F (normal rat kidney cells, ATCC®), was cultivated with a culture medium in a culture flask (75 cm^2, Corning®), which was kept in an incubator at 37 ℃ and 5% CO_2. The cell culture medium contained Dulbecco's Modification of Eagle's Medium (DMEM, Mediatech, Inc.), 5% fetal calf serum (FCS, Materials Bio Inc.), and 1% penicillin-streptomycin (PSN, Mediatech, Inc.). The fibroblasts were selected for seeding on meshes to investigate their biocompatibilities because they play a basic role in the process of foreign body reaction and collagen synthesis [52].

3.3 Formation of Vital/avital Composite Mesh

Prosthetic mesh was sterilized by soaking in 70% (v/v) ethanol for 20 mins, and then by treating for 2 h with phosphate buffered saline (PBS) containing 1% PSN. The sterilized mesh was soaked into 700 µl culture medium in a culture dish (Ø 60 mm × 15 mm, Corning®) before it was brought in contact with cells.

The confluent NRK-49F cells were trypsinized in a culture flask and suspended to create a cell suspension at a concentration of 3×10^6 cells/ml. Cell number was determined by hemacytometer counting plate (Bright-Line™). A 3 ml cell suspension was added in each culture dish to seed on the mesh. The culture dish was kept in an incubator at 37 ℃ and 5% CO_2 in order to support cell growth. The culture medium was replaced every three days and the vital/avital composite meshes formed after seven-days incubation. The mesh soaked in culture medium without cells was used as a control. To prevent contamination of cell cultures, all steps of the experiment were carried out under sterile conditions.

3.4 Biocompatibility of Prosthetic Hernia Mesh

The cell morphology and cell proliferation after contact with different prosthetic meshes are primary methods to qualitatively and quantitatively investigate the bicompatibility of meshes in *in vitro* studies [14, 53-55].

3.4.1. Cell morphology

The micrographs of the vital/avital composite meshes were taken using environmental scanning electronic microscopy (ESEM, Zeiss 1450EP, MicroImaging, Inc.). The ESEM is a type of electron microscope that can produce a very high-resolution image of a sample surface, revealing details of 1 to 5 nm. The vital/avital composite meshes were rinsed by PBS, and fixed in 80% (v/v) acetone solution at -20 ℃ followed by Aurum sputtering for 1 min before examining in the ESEM.

3.4.2. Cell proliferation

MTT (3-(4,5-dimethylthiazol-2yl)-2,5-diphenoltetrazolium bromide) test was used to quantitatively investigate the cellular response of fibroblasts after contact with different meshes. It is a colorimetric test to determine the proliferation of vital cells. The light yellow MTT was transferred to the deep blue crystals of formazan by the mitochondrial metabolism of vital cells. The formazan crystals then were dissolved in a dimethyl sulfoxide (DMSO) solution and be photometrically measured at 570 nm.

NRK-49F cells at a concentration of 5×10^5 cells/well were preincubated with previously described medium in a 6-well plate (Multiwell™, Becton Dickinson) until a confluence of 80% was achieved. Further, after incubation in 0.1% FCS-containing medium for 24 h, cells were kept in contact with different meshes in a FCS-free medium. A mesh-free cell suspension was used as a control. After an incubation of 72 h, a 30 µl MTT solution (0.5 mg/ml) was added to each well

and the plate was incubated for 4 h at 37 ℃, 5% CO_2. A 3 ml DMSO solution was then added to dissolve the formazan crystals. The dissolved formazon solution was added into 96-well plate and spectrophotometrical absorbency was measured as the value of optical density (OD) at 570 nm wavelength by using an ELISA reader (Synergy HT, Bio Tek Instruments, Inc.). The OD value was linearly related to the number of vital cells. The difference in the OD value of the mesh containing medium and the control illustrated the increase or decrease in cell proliferation that was induced by prosthetic mesh. Each specimen had five replications. The results were statistically tested by ANOVA with a confidence level of .05.

3.5 Mechanical Response of Prosthetic Hernia Mesh

After seven-day cell incubation, the vital/avital composite mesh was transferred to dynamic mechanical analyze (DMA 8000, PerkinElmer, Inc.), as shown in *Figures 3.1a*, to investigate the mechanical response of hernia meshes under *in vitro* condition. Time-independent and time-dependent mechanical behaviors of the composite are commonly used methods to identify and predict the mechanical properties of biomaterials during their lifetime use [47].

3.5.1. Time-dependent tensile behavior

The tensile performance of the vital/avital composite meshes and their controls without cell incubation were conducted by DMA at 37 ℃ to investigate the time-independent mechanical response. The samples were loaded at 0.2 N/min and the corresponding strains were measured. The elastic modulus (MPa) and ultimate strength (KPa) of samples were calculated from their stress-strain curves to determine mechanical properties. The elastic modulus is the linear ratio between stress and strain, and the ultimate strength is defined as the maximum loading force

divided by the cross-sectional area of samples. Each specimen had three replications. The results were statistically tested by student t-test with a confidence level of .05.

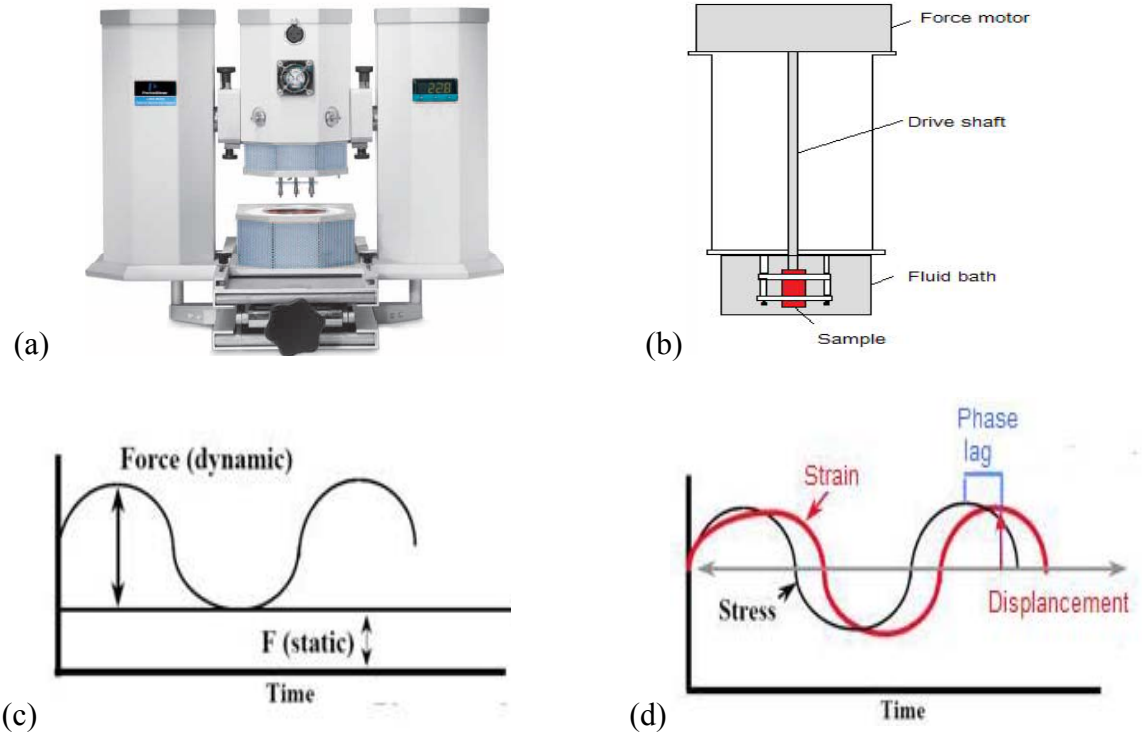

Figure 3.1 Schematic of mechanical simulation. (a) DMA with fluid bath, (b) schematic of the DMA in tension geometry, (c) sample is subjected to a sinusoidal oscillating stress, (d) sample's response in terms of strain wave within elastic limits.

3.5.2. Time-dependent dynamic mechanical simulation

Dynamic mechanical simulations were carried out by DMA to investigate the time-dependent behaviors of the vital/avital composite meshes. *Figure 3.1b* illustrates the sample mounting under tension geometry in DMA for simulation experiment. The fluid bath was filled with the same culture medium. The temperature of the fluid bath was maintained at 37 ℃ during the entire simulation. The force motor controls to generate a sinusoidal oscillating stress which

transmits to the sample via a drive shaft. *Figure 3.1c* illustrates the applied force to the sample as a function of time, which can be written as *Equation 3.1*. The sample's response, as shown in *Figure 3.1d*, in terms of sinusoidal strain had the phase lag due to its viscoelasticity. The strain at any time can be written as *Equation 2*.

$$\sigma(t) = \sigma_0 \sin(\omega t) \tag{3.1}$$

where $\sigma(t)$ is the stress at anytime, σ_0 the maximum stress, ω the frequency of oscillation, and *t* the time

$$\varepsilon(t) = \varepsilon_0 \sin(\omega t + \delta) \tag{3.2}$$

where $\varepsilon(t)$ is the strain at anytime, ε_0 the strain at maximum stress, ω the frequency of oscillation, *t* the time, and δ the phase angle.

The vital/avital composite meshes and their controls were mounted on tension geometry with a 1 N pretension to keep them under taut conditions. During the simulation experiment, these meshes were subjected to a sinusoidal strain of 0.05 Hz for a resting phase of 3 h, and then the frequency was increased to 0.5 Hz to establish the active phase simulation for 1 h. The amplitude of the sinusoidal strain was 150 μm, which corresponds to the 2% strain. The storage modulus (E') of sample was continuously measured during dynamic simulations. The storage modulus (also called the in-phase modulus or the real modulus) is a measurement of the elastic response of a viscoelastic material, indicating the stiffness of sample [56]. The storage modulus can be determined using *Equation 3.3*.

$$E' = (\sigma_0/\varepsilon_0)\cos\delta = (f_0 L_0/A_0\, K)\cos\delta \quad (3.3)$$

where E' is the storage modulus, f_0 the force applied at the peak of the sinusoidal wave, K the sample displacement at the peak, δ the phase angle, L_0 the original length of the sample, and A_0 the original cross-sectional area through which the force is applied.

The entire dynamic simulation for each specimen was conducted for 11 h, in which three resting phases followed two active phases, to determine the time-dependent mechanical behavior. The composite mesh had three replications of dynamic mechanical simulations, whereas its control was only subjected to the simulation experiment once. The average storage modulus from each simulation phase (resting or active) was calculated to reflect the change in mechanical response during the dynamic simulation.

CHAPTER 4

RESULTS AND DISCUSSION

4.1 Major Properties of Prosthetic Hernia Mesh

Polypropylene (PP), polyester (PET) and polytetrafluoroethylene (PTFE) meshes are the clinical biomaterials which are widely used for the repair of abdominal wall defects. Major physical and mechanical parameters of all studied prosthetic hernia meshes were summarized in *Table 3.1*. All meshes were made by knit construction because it prevents the edges of the mesh from unraveling when being cut in surgery. These were macroporous meshes containing pore sizes larger than 75 μm, which is the required pore size to allow macrophages, fibroblast and collagen fibers to penetrate, growth and differentia [57].

The PP601, PET, and PTFE meshes were all heavyweight (>95 g/m^2); however, they showed significantly different mechanical properties. Although the PP601 and PTFE meshes were made of doubled filaments with the same diameter (150 μm), the PP601 mesh had a bursting strength of 1063 N, nearly twice that of the PTFE mesh. The PP601 mesh was the stiffest (elastic modulus of 11.89 MPa) and appeared quite rigid while cutting, whereas the PTFE mesh was very supple and flexible with an elastic modulus of 3.67 MPa. The increase in compliance makes the PTFE mesh more closely matched with the elasticity of the abdominal wall; however, it could render the mesh difficult for surgeons to handle or manipulate in the operating room. The PET mesh was made of multifilament polyester, whose structure was generally less stiff and more pliable, but it probably increased the surface area of contact with

surrounding tissues. The filaments of the PET mesh were much thinner (20 μm in diameter) than those of the PP and PET meshes. The interstices between these filaments were less than 10 μm, providing a suitable housing for bacterial growth because they allow bacteria to penetrate but prevent macrophages from attacking them. For this reason, the multifilament PET mesh is potentially at high risk of postoperative infection after implantation in the recipient.[57]

Two lightweight PP403 and PP404 meshes (<45 g/m^2) were compared with heavyweight PP601 mesh to investigate the influence of mesh weight on biocompatibility and mechanical properties of PP hernia meshes. They produced using thinner filament yarn (100 μm in diameter) than the heavyweight mesh. The PP403 mesh had doubled filaments, whereas the PP404 mesh consisted of monofilaments. This reduction of material density gives lightweight mesh a small surface area of contact with the host tissues. Lightweight meshes have shown lower mechanical strength and stiffness. The PP404 mesh demonstrated the weakest mechanical properties (510 N in bursting strength) among all meshes; however, it exceeded the normal forces (~232 N) acting on the abdominal wall fascia.[9] Therefore, all studied meshes were able to provide enough mechanical performance to support the abdomen wall.

4.2 Cell Incorporation of Prosthetic Hernia Meshes

Cell cultures have been useful for testing the biocompatibility of biomaterials [51]. Different cell morphology of fibroblasts on the hernia mesh illustrated the cell incorporation with mesh, which was commonly used method to predict the mesh integration within host tissues during *in vitro* studies [55, 58].

4.2.1 The influence of mesh materials

After seven-days culture on the PP601 mesh, NRK-49F cells distributed randomly on the surface of filaments (*Figure 4.1a*). The morphologic aspect of the cells was connective and mainly orientated parallel to the filaments. Few cells were confined to the interstices between filaments.

For PET mesh (*Figure 4.1b*), NRK-49F cells also grew randomly on entire mesh after seven-days of incubation, but there was more cell growth in the crevasses of the filaments rather than on the surface of the single filament. Hence, a network structure of cells formed inside the bundle of filaments.

After a week of growth with PTFE mesh, NRK-49F cells preferred to loosely accumulate on certain areas of PTFE filaments, rather than dispersing on the entire mesh (*Figure 4.1c*). The cellular morphology was tangled up along the lateral direction of the filaments rather than being orientated along the filaments.

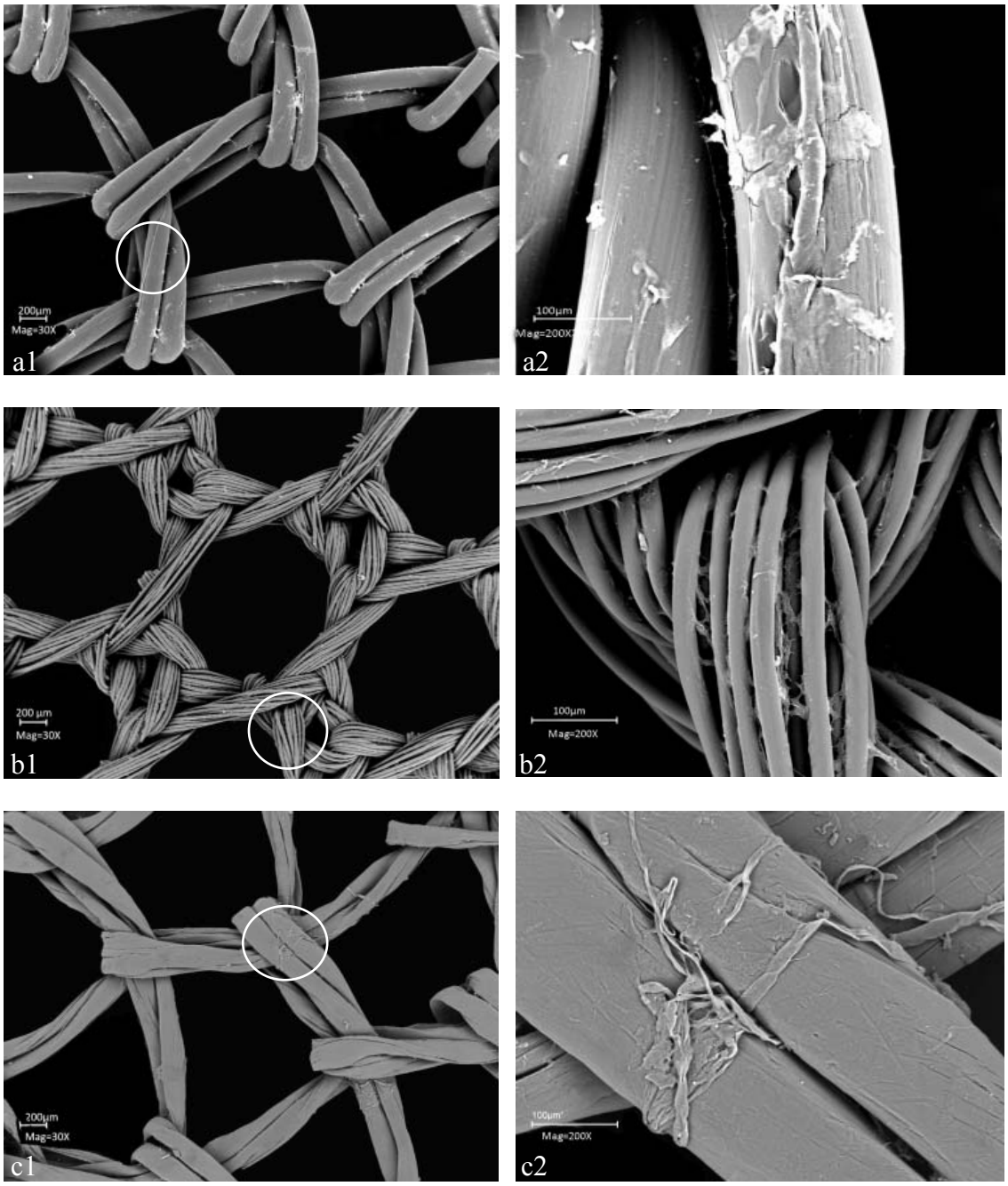

Figure 4.1 SEM images of heavyweight vital/avital composite meshes: a) PP601 mesh, b) PET mesh, c) PTFE mesh cultured with NRK-49F cells for seven days. The scale bar stands for 200 µm in a1, b1, c1 and 100 µm in a2, b2, c2.

Generally, the cell morphology of fibroblasts cultured on the meshes illustrated the mesh incorporation with fibroblasts, which is the critical factor for determination the mesh integration into the host tissues after implantation. This is because fibroblasts are primary components of the cellular layer between biomaterials and the connective tissues, and effective wrapping by the cellular layer allows implanted mesh to further integrate into the recipient tissues [59]. In the present study, the PP and PET meshes exhibited better cellular incorporation with fibroblasts than PTFE mesh because the cell growth was more extensive and firmly attached to them. This difference in the behavior of the fibroblasts can be result of the surface tensions of biomaterials. The polymeric materials of higher critical surface energy stimulates higher spreading and proliferation of cells. A low critical surface tension of PTFE (18.5 dyn/cm) [60-61], which is difficult for cell to attach and grow on the surface is responsible for the lack of cell growth on PTFE mesh. However, the critical surface tension for monofilament PP fiber is 39 dyn/cm [62] and that of PET fiber is 43 dyn/cm [63], resulting in better cellular incorporation and corresponding tissue integration than the PTFE mesh. The lack of cell and tissue incorporation with the PTFE mesh was found to cause the high recurrence rates after macroporous PTFE mesh implantation in clinical studies [38]. For this reason, the microporous PTFE mesh (ePTFE) is developed to induce more cell and tissue ingrowth because the small pores impairs fluid transport that causes an accentuated cell/tissue response in the host [64].

4.2.2. The influence of mesh weights

Similar to heavyweight PP601 mesh in *Figure 4.1a*, NRK-49F cells also extensively distributed on lightweight PP403 and PP404 meshes. Regarding the PP403 mesh, the cells grew along the filaments and were more likely to form an organized layer wrapping the mesh (*Figure 4.2a*). With regard to the PP404 mesh, the fibroblasts growth on the straight filaments were

isolated and single cells, but the cells preferred to connectively grow around the mesh nodes, forming a wrapping layer (*Figure 4.2b*).

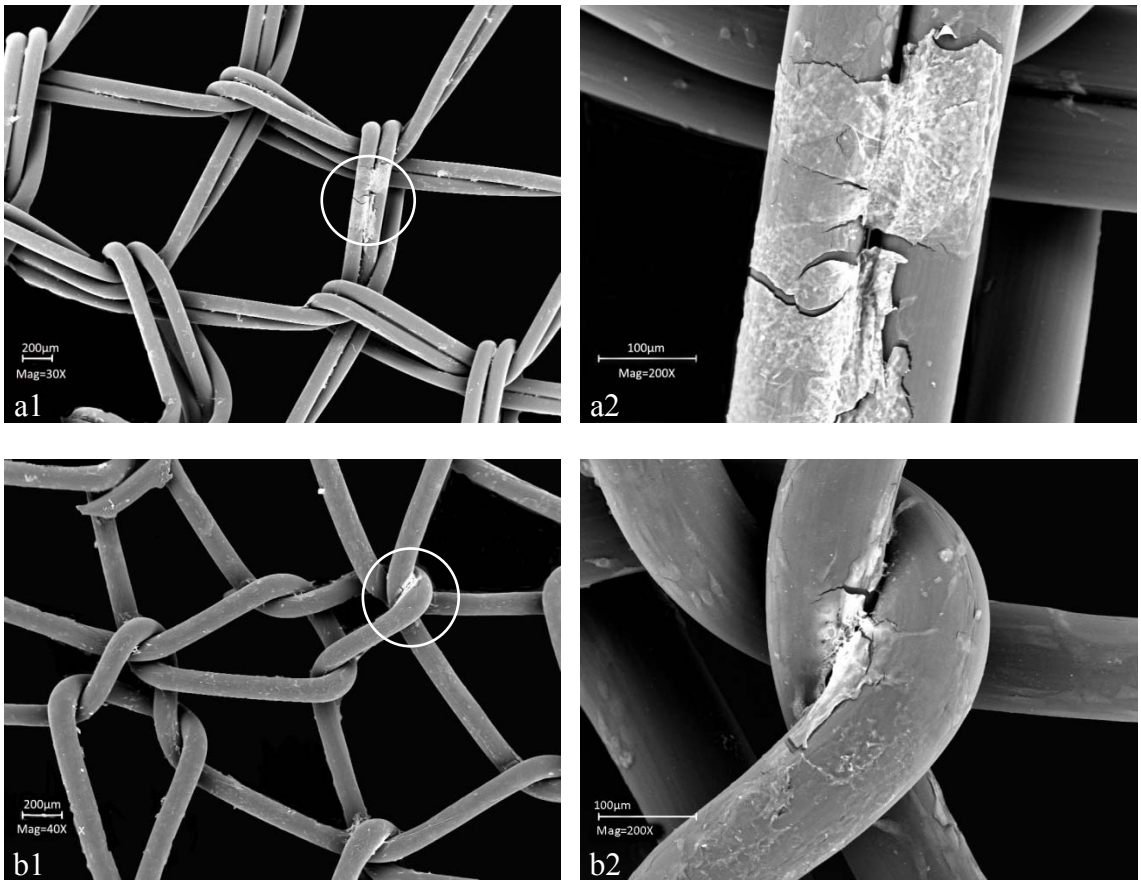

Figure 4.2 SEM images of lightweight vital/avital composite meshes: a) PP403 mesh, b) PP404 mesh cultured with NRK-49F cells for seven days. The scale bar stands for 200 µm in a1, b1 and 100 µm in a2, b2.

Although the prosthetic mesh repair pronouncedly decreases the recurrence rate of hernia repair, it causes considerable pain and increased stiffness around the abdomen, according to some clinical reports [8-10]. This has led to various types of mesh being studied and engineered. Regardless of mesh materials, the weight of an implanted mesh has become the most discussed parameter. Some studies have demonstrated that newly developed meshes have decreased weight

to reduce the foreign body response and resulted in better tissue incorporation and less stiffness of abdomen [9, 13, 65]. However, other studies questioned the leading role of material amount and argued that other parameters such as pore size and fibrous structure might be of importance for biological response of imported meshes [14-16]. In the present study, it was shown that the lightweight PP403 mesh using thinner filaments resulted in better cellular incorporation, whereas the lightweight PP404 mesh, with monofilament rather than doubled filaments, decreased the extent of mesh incorporation into cells. These different extents of cellular incorporation were caused by different surface areas of meshes exposed to the cells. Therefore, mesh weight and structure both will exert important influence on mesh incorporation into the host cells and tissues after implantation.

4.3 Initial Foreign Body Reaction of Prosthetic Hernia Mesh

The proliferation of fibroblasts is an important growth factor in the inflammatory reaction because the number of fibroblasts is significantly and directly correlated with the quantity of inflammatory cells (macrophages and polymorphonuclear leucocytes) [11]. Hence, the cellular proliferation of fibroblasts caused by different meshes was used to predict the initial foreign body reaction after mesh implantation in *in vitro* studies [14-15].

The MTT test (*Figure 4.3*) demonstrated the significant differences in cell proliferations after fibroblasts contacting with different prosthetic meshes, compared with control group in which the cells grew in mesh-free medium. Overall, the proliferation of NRK-49F cells was stimulated by PP and PET meshes, but suppressed by the PTFE mesh. All PP meshes significantly induced more cell growth than the PET mesh ($p < .05$). The most cellular proliferation was caused by the heavyweight PP601 mesh. The lightweight PP mesh (PP403 and

PP404) showed significantly less growth induction than the heavyweight PP mesh ($p < .05$). There was no significant difference in cell proliferation between PP403 and PP404 meshes.

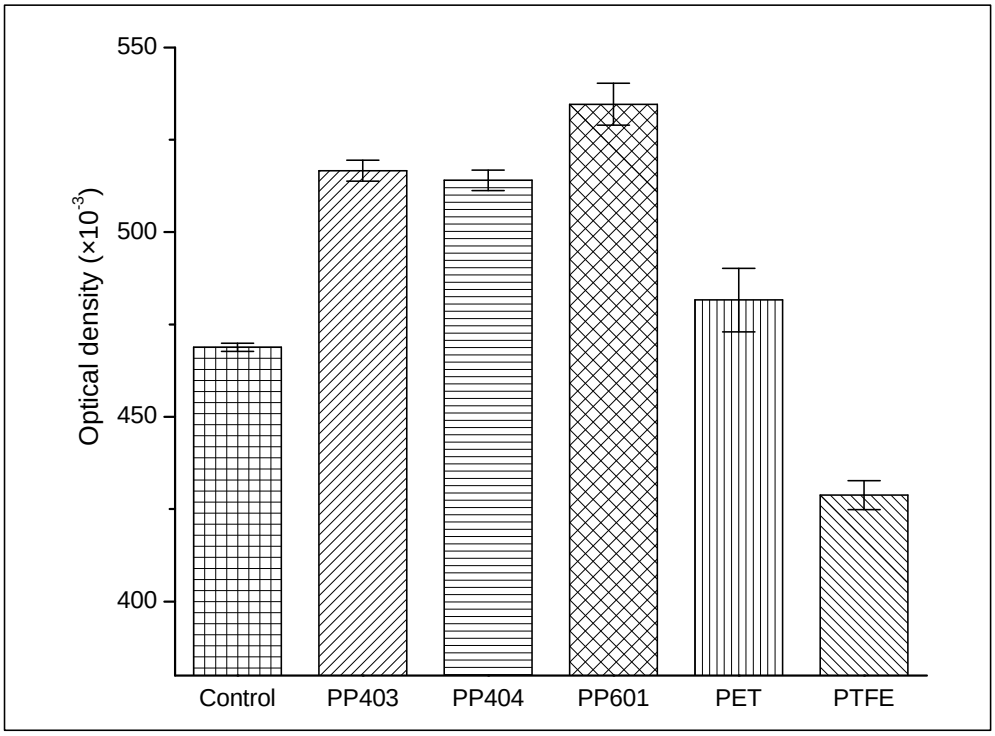

Figure 4.3 Optical density (OD) of formazan solution to determine cell proliferation of NRK-49F cells after contacting with different prosthetic meshes. Note: the OD was significantly increased by PP and PET meshes, but significantly decreased by PTFE mesh, compared with the control ($p < .05$). The PP meshes had larger increase in OD than that of PET mesh, and heavyweight PP601 mesh induces the most increase ($p < .05$). Error bar stands for standard deviation (SD). Five replications for each specimen.

The experimental results suggested that the mesh materials and weights determined the growth behavior of cells and would elicit different extents of initial foreign body response in the recipient. PP and PET meshes would induce the acute initial inflammatory reaction, whereas the

PTFE mesh would present a weaker foreign body reaction. Many studies have demonstrated that some synthetic biomaterials induced an acute inflammatory reaction, which was regulated by their chemical nature and physical features, but the correlation has not been fully understood [11, 66-67]. Regardless of physical parameters, the chemical compounds of polymer chain may control the stimulation and migration of inflammatory cells, resulting in different extents of inflammatory reaction at implanted sites [63]. The acute foreign body reaction to PP and PET meshes in the early period were found in *in vivo* studies [11-12], and the result regarding the inflammation of PTFE mesh in this study was also in concordance with their reports. According to Marois et al. [68], the initial acute inflammatory reaction after implantation stimulated the growth of surrounding cells and tissues in the early stage. This is another reason why PP and PET meshes have better cell incorporation than PTFE mesh in our studies.

The influence of mesh weight on the initial inflammatory response in the recipient was also investigated in *in vitro* study. Lightweight meshes (PP403 and PP404) induced less cell proliferation than the heavyweight PP601 mesh, which illustrated that material reduction either by changing knit structure or by the use of thinner fiber weakened the foreign body reaction. This is because lightweight mesh has a smaller mesh-cell/tissue interface than heavyweight mesh, and thus may induce less inflammatory reaction at the implanted sites. This finding was consistent with other investigations in describing an acute foreign body reaction for heavyweight polypropylene meshes [9-10, 69]. For mesh materials with acute inflammation, it is critical to reduce the inflammatory reaction because it causes reduced compliance of the abdomen and shrinkage of mesh [9]. Heavyweight PP mesh creates an intense inflammatory response that leads to the rapid cell proliferation. This excessive cell growth tends to form an unorganized and thick cellular layer on PP mesh that may cause the contraction of mesh. However, lightweight PP

mesh reduces the inflammatory response and decreases the degree of unorganized cell growth that may improve the tissue incorporation. Therefore, in the present study, the cell morphology on lightweight meshes was preferable for forming a uniform cellular layer that wrapped the filaments well.

4.4 Mechanical Properties of Vital/avital Composite Mesh

The biomechanical properties of prosthetic mesh after implantation are of significant importance because the primary function of hernia mesh is to provide mechanical support to the ruptured abdominal wall. The mechanical failure of implanted mesh is responsible for some serious postoperative complications, such as “stiff abdomen” and recurrence of hernia.

4.4.1 Tensile behavior of vital/avital composite mesh

Time-independent behaviors of the vital/avital composite meshes and their controls without cell incubation were measured by stress-strain curves of tensile testing, where the true strain (logarithmic strain) was used due to the ductile nature of samples [47], as shown in *Figure 4.4*. The stiffness (elastic modulus) of sample refers to the linear ratio between stress and true strain, and the ultimate strength of sample is defined as the maximum force divided by the specimen cross-sectional area. *Figure 4.5* and *Figure 4.6* summarize the elastic modulus and the ultimate strength for all studied composite meshes and their controls.

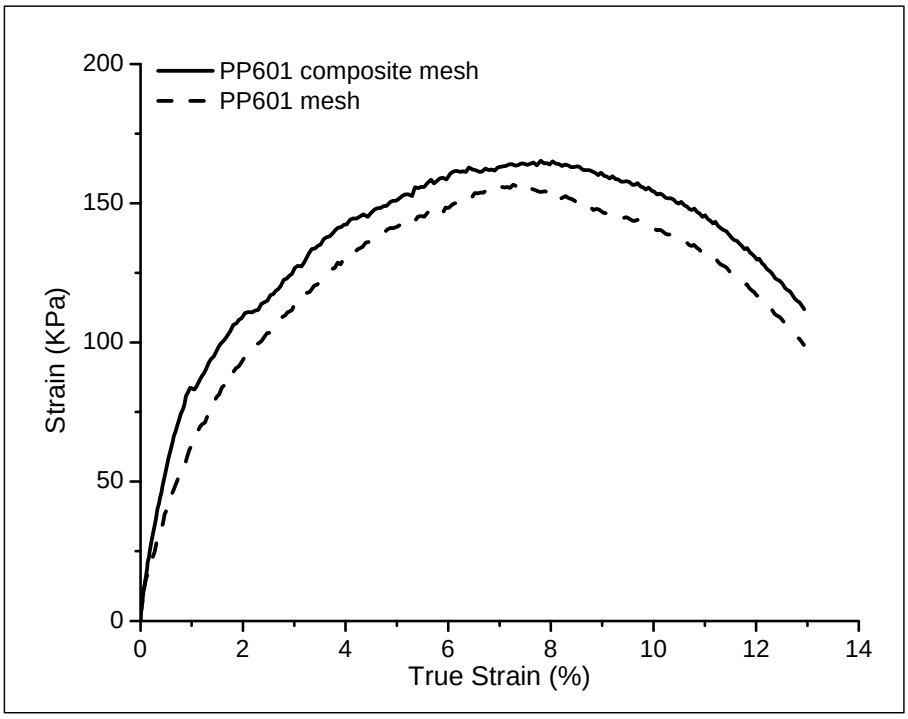

Figure 4.4 Tensile stress-strain curve of PP601 mesh and its vital/avital composite mesh.

As far as elastic modulus (*Figure 4.5)*, all vital/avital composite meshes were stiffer than their controls, but the stiffness increase was only statistically significant in the heavyweight PP 601 and PET meshes ($p < .05$). The stiffness of PET mesh increased nearly two times and the PP601 mesh exhibited a 50% increase in stiffness. However, PTFE and lightweight (PP403 and PP404) composite meshes only exhibited 20% increase in mean stiffness. The cellular incorporation with mesh caused its increase in stiffness, and the various cell morphologies led to different extents of stiffness change. The better cell incorporation of PP601 and PET meshes led to more stiffness increase than the PTFE mesh. The PET mesh demonstrated the largest extent of stiffness increase because there was more possibility for cell to grow in the crevasses of polyester filaments, forming the cellular network structure. Moreover, lightweight meshes

(PP403 and PP404) induced weak inflammatory response and well organized cellular morphology, implying less increase in stiffness than heavyweight PP601 mesh.

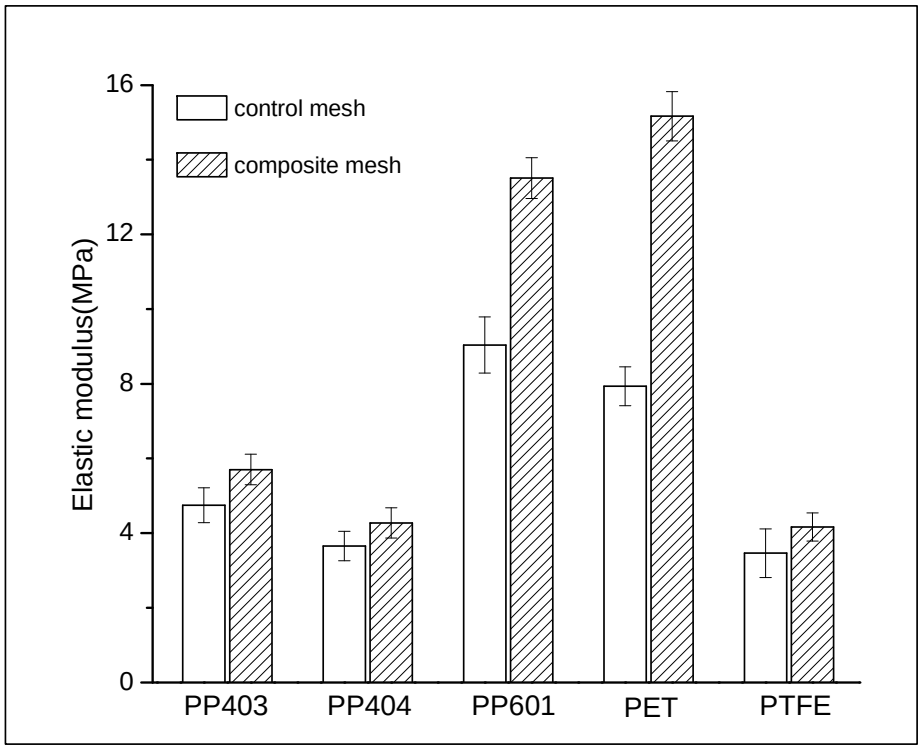

Figure 4.5 Elastic modulus of vital/avital composite mesh compared with its control (without cells). Note: all composite meshes had increase in elastic modulus, but the increase was only statistically significant in PP601 and PET meshes ($p < .05$). Error bar stands for SD. Three replications for each specimen.

The ultimate strength, shown in *Figure 4.6*, significantly increased in all PP and PET meshes after incubation with cells ($p< .05$), but significantly decreased in PTFE composite mesh ($p< .05$). Lightweight PP403 and PP404 meshes had more increase (25%) in ultimate strength than heavyweight PP601 and PET meshes, in which the PP601 mesh had 6% increase and the

PET 14%. The cell incorporation with PP and PET meshes caused the increase in ultimate strength, which will contribute to mechanical reinforcements of meshes after implantation in the host. However, the less cell growth on PTFE mesh resulted in failure of its mechanical reinforcement. The reason for the strength decrease of PTFE composite mesh requires further studies. Lightweight meshes gained larger mechanical reinforcement from cell incorporation when compared to heavyweight meshes, because they have less mechanical strength before culturing with cells. Therefore, the adequate cell incorporation with meshes would help them to reinforce mechanical strength after implantation in the recipient, especially lightweight meshes.

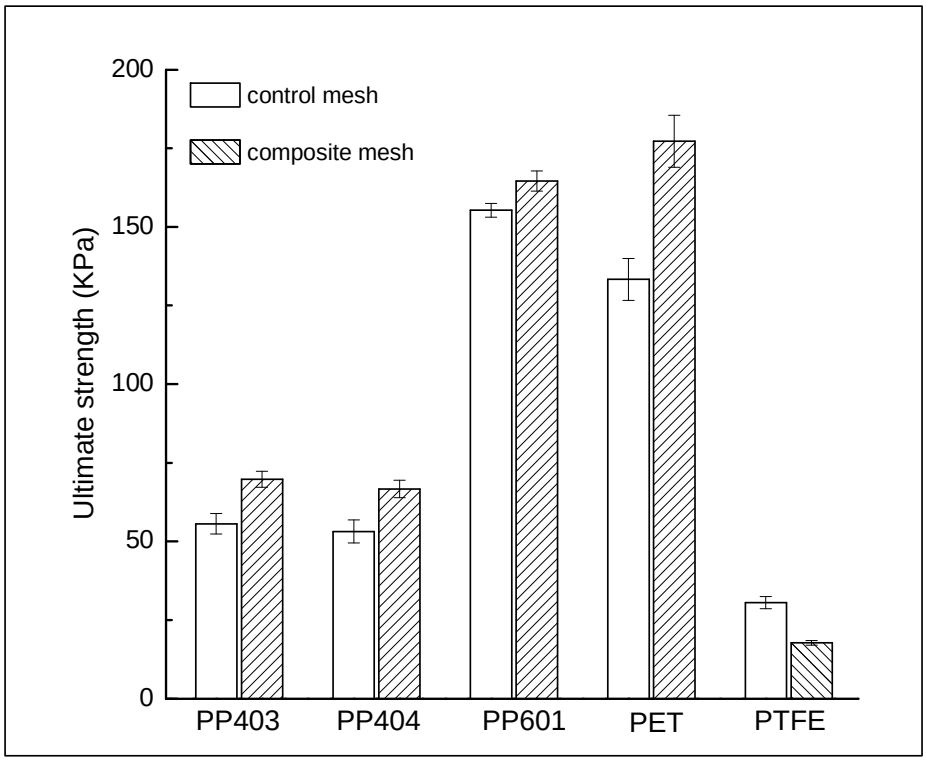

Figure 4.6 Ultimate strength of vital/avital composite mesh compared with its control (without cells). Note: PP and PET composite meshes showed significant increase in ultimate strength, whereas PTFE composite mesh had significant decrease in ultimate strength ($p <$ .05). Error bar stands for SD. Three replications for each specimen.

4.4.2. Dynamic mechanical simulation of vital/avital composite mesh

The dynamic mechanical simulation was conducted to investigate the time-dependent behaviors of prosthetic meshes, which can be used to predict long-term mechanical properties of the implant. The simulation experiment ran over 11 h in which the storage modulus, indicating stiffness of sample, was measured over simulation period (*Figure 4.7*).

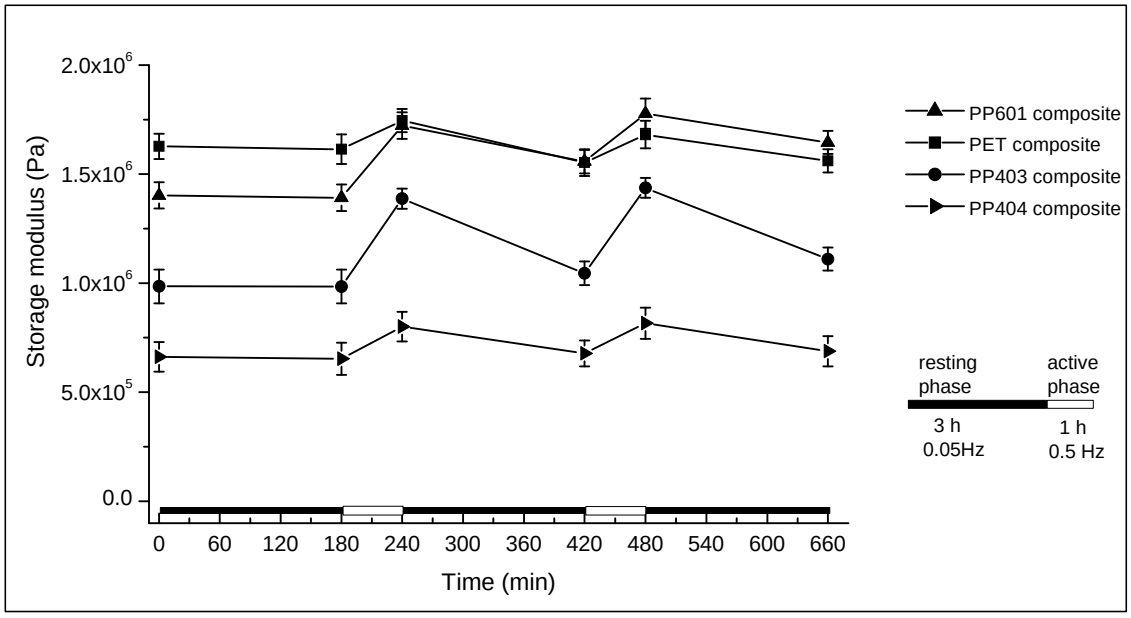

Figure 4.7 Storage modulus of vital/avital composite mesh during dynamic mechanical simulation. Note: the average data points from each simulation phase (resting and active) were connected to show time-dependent behavior of vital/avtial composite mesh. The black and white bar on x-axis represents the resting and active phases. Error bar stands for SD. Three replications for each specimen.

The results of the simulation experiment illustrated that the stiffness of vital/avital composite decreased during the resting phase with 2% strain at .05 Hz and the subsequent active phase with 2% strain at 0.5 Hz led to an increase in stiffness (*Figure 4.7*). PTFE mesh was not subjected to the dynamic simulation experiment due to its weak mechanical stability under dynamic loading. The increase in stiffness during active phase can be due to the growth of incorporated cells that was stimulated by accelerated dynamic mechanical force. The composite meshes exhibited different overall changes in stiffness after entire simulation (*Figure 4.8*). An overall gain in stiffness was observed in all PP composite meshes, whereas PET composite showed a slight overall loss (-4.1%) in the stiffness. PP601 composite (17.3%) had the significantly larger percent change of stiffness than PP403 (12.7%) and PP404 (4.0%) composites. However, the stiffness of meshes without cell growth continuously reduced during dynamic simulation (*Figure 4.8*). The decrease in stiffness for all tested samples was caused by the stress relaxation of materials under dynamic stretching. Viability of cells distributed on the composite mesh was checked qualitatively by SEM after entire simulation and no significant cell loss was found in stimulated samples when compared to the unstimulated ones.

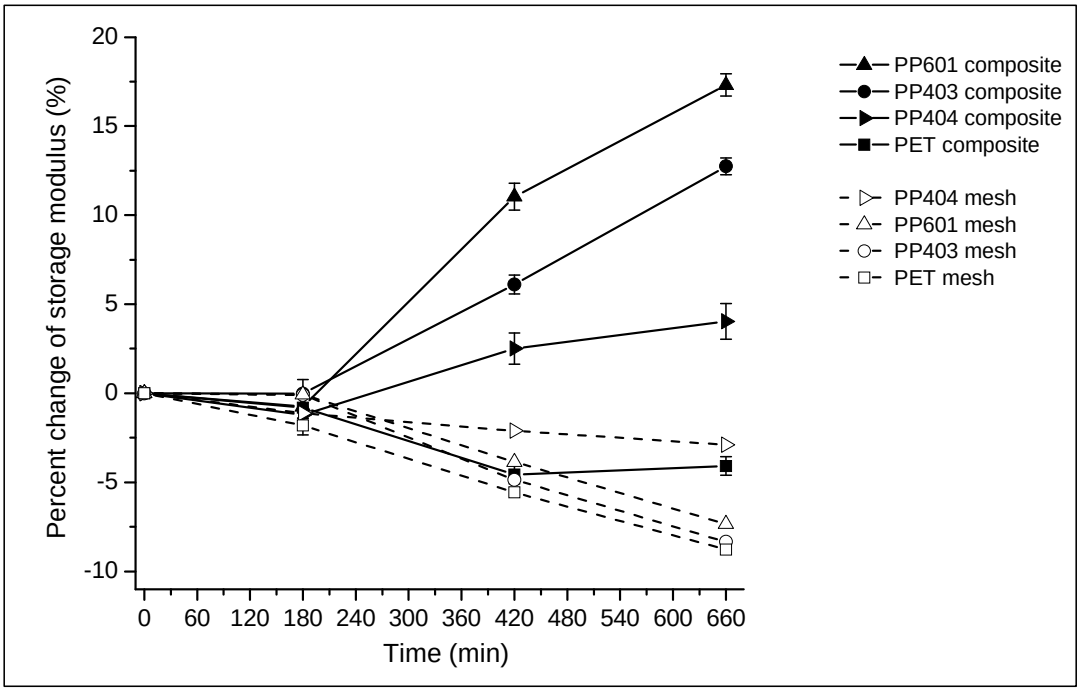

Figure 4.8 Percent change of storage modulus of mesh and it vital/avital composite during dynamic mechanical simulation. Note: the average storage modulus at resting phase was compared with initial storage modulus to show mechanical change after entire simulation experiment. Error bar stands for SD. Three replications for vital/avital composite.

The time-dependent behaviors of different prosthetic hernia meshes have been investigated in *in vitro* studies to predict their long-term mechanical properties. According to the present study, we predict that the stiffness of PP meshes will exhibit an increasing trend, whereas the stiffness of the PET mesh will decrease after gaining an increase in initial stiffness by cell incorporation. This prediction is supported by the cause of the most serious complication associated with heavyweight PP mesh; that is, an increased stiffness after implantation of heavyweight PP mesh resulted in reduced compliance of the abdominal wall, dubbed “stiff abdomen” [9]. The degradation of PET mesh may cause its overall loss in stiffness after

simulation experiment. A large gain in initial stiffness is critical for PET hernia mesh because the increase could make up for the long-term decrease in stiffness of the mesh and thus maintain its mechanical stability in the recipient. For this reason, PET hernia meshes are usually made of multifilament structure to stimulate more cell growth, leading to a larger initial increase in stiffness. The weight reduction of the PP mesh reduces its increase in stiffness in the long term because lightweight mesh not only is more compliant, but also weakens the initial foreign body reaction, resulting in a smaller initial increase in stiffness after implantation. However, some lightweight meshes are too flexible to handle during surgery, and hence the composite mesh combining polypropylene with the absorbable components such as polyglactin was developed to prevent increase in stiffness as the absorbable materials gradually dissolved in the host [9]. Moreover, the mesh integrated with cells inhibited the mechanical loss when compared with mesh without cells during dynamic simulation. Therefore, adequate mesh incorporation into cells or tissues is critical for maintaining its mechanical integrity after long-time implantation.

CHAPTER 5

CONCLUSIONS AND FUTURE WORK

5.1 Conclusions

The influence of mesh materials and weights on the biological response and mechanical properties of hernia meshes after implantation was investigated in an *in vitro* model by growing NRK-45F cells on different prosthetic hernia meshes.

Regarding the biological responses, the PP and PET meshes induced an acute initial foreign body reaction, implying better cell incorporation than the PTFE mesh. This will contribute to the better integration of the PP and PET meshes into host tissues after implantation in the recipient. With the same materials (e.g., PP), incorporation of the mesh with cells was influenced by the weight and structure of the mesh. Weight reduction seems to be an effective way of weakening the foreign body reaction induced by PP biomaterials because of the smaller mesh–cell/tissue interface in the host.

With regard to mechanical properties, the cell incorporation significantly increased the stiffness of the heavyweight PP and PET hernia meshes. The weight reduction of the PP mesh could inhibit the extent of increase in stiffness and reduce the complication of “stiff abdomen” in the long term. Moreover, cell incorporation also contributed to the mechanical reinforcements and could ensure the mechanical integrity of the implant in long-term implantation.

5.2 Future Work

On the basis of work that was conducted in this study, the author would like to propose following future studies:

1) Other constructional parameters of prosthetic mesh besides mesh weight, such as pore size and fibrous structure, should be investigated to study their influence on morphology of cells cultured on the mesh.
2) The other changes in behavior of cells when they contact prosthetic meshes, such as the rate of apoptosis and cell invasion, may provide additional information that will contribute to better understanding of the biological response to the meshes.
3) The reason why the ultimate strength of PTEF composite mesh decreased requires further studies. The thermal analysis (TGA and DSC) or FTIR spectroscopy would be conducted to investigate changes in weight loss, oxidation or degradation of prosthetic mesh after culturing with cells.
4) Further *in vitro* studies on a wider range of meshes, such as ePTFE, PP/absorbent materials, could be carried out to define the best combination of material and constructional characteristics required for a mesh implant to assure adequate biocompatibility and long-term mechanical stability.
5) Considering the limitation in *in vitro* studies, one-dimensional models fail to represent the complexity of tissue and whole organism biological response, the animal experiments in *in vivo* are suggested to be conducted to substantiate the results of *in vitro* cell culture studies.

REFERENCES

1. Kingsnorth, A., *Treating inguinal hernias.* British Medical Journal, 2004. **328**: p. 59-60.
2. Turaga, K., R. Fizgibbons Jr, and V. Puri, *Inguinal Hernias: Should We Repair?* Surgical Clinics of North America, 2008. **88**: p. 127-138.
3. Scott, N. and P. Gragam, *Open mesh versus non-mesh for groin hernia repair.* Cochrane Database of Systematic Reviews, 2001. **3**: p. CD002197.
4. Klinge, U., J. Conze, and B. Klosterhalfen, *Changes in abdominal wall mechanics after mesh implantation. Experimental changes in mesh stability.* Langenbecks Arch Chir, 1996(381): p. 323-332.
5. Klosterhalfen, B., U. Klinge, U. Henze, R. Bhardwaj, J. Conze, S. J.P., C. Ackermann, and P. Tondelli, *Preperitoneal prosthesis implantation in surgical management of recurrent abdominal wall mechanics after mesh implantation.* Langenbecks Arch Chir, 1997(382): p. 87-94.
6. Ghadimi, B.M., C. Langer, and H. Becker, *The carcinogenic potential of biomaterials in hernia surgery.* Chirurg, 2002(73): p. 833-838.
7. Weyhe, D., O. Belyaev, C. Müller, K. Meurer, K.-H. Bauer, G. Papapostolou, and W. Uhl, *Improving outcomes in hernia repair by the use of light meshes--a comparison of different implant constructions based on a critical appraisal of the literature.* World Journal of Surgery, 2007. **31**(1): p. 234-244.

8. Klinge, U., B. Klosterhalfen, M. MÃ¼ller, A.P. Ottinger, and V. Schumpelick, *Shrinking of polypropylene mesh in vivo: an experimental study in dogs.* The European Journal Of Surgery = Acta Chirurgica, 1998. **164**(12): p. 965-969.

9. Cobb, W.S., K.W. Kercher, and B.T. Heniford, *The argument for lightweight polypropylene mesh in hernia repair.* Surgical Innovation, 2005. **12**(1): p. 63-69.

10. Cobb, W.S., J.M. Burns, R.D. Peindl, A.M. Carbonell, B.D. Matthews, K.W. Kercher, and B.T. Heniford, *Textile Analysis of Heavy Weight, Mid-Weight, and Light Weight Polypropylene Mesh in a Porcine Ventral Hernia Model.* Journal of Surgical Research, 2006. **136**(1): p. 1-7.

11. Klinge, U., B. Klosterhalfen, M. MÃ¼ller, and V. Schumpelick, *Foreign body reaction to meshes used for the repair of abdominal wall hernias.* The European Journal Of Surgery = Acta Chirurgica, 1999. **165**(7): p. 665-673.

12. Gonzalez, R. and B.J. Ramshaw, *Comparison of tissue integration between polyester and polypropylene prostheses in the preperitoneal space.* The American Surgeon, 2003. **69**(6): p. 471-476.

13. Dirk, W., S. Inge, B. Orlin, G. Robert, M. Klaus-Michael, U. Waldemar, and Z. Volker, *Experimental Comparison of Monofile Light and Heavy Polypropylene Meshes: Less Weight Does Not Mean Less Biological Response.* World Journal Of Surgery, 2006. **30**(8): p. 1586-1591.

14. Weyhe, D., O. Belyaev, G. Buettner, K. Mros, C. Mueller, K. Meurer, G. Papapostolou, and W. Uhl, *In vitro comparison of three different mesh constructions.* ANZ Journal Of Surgery, 2008. **78**(1-2): p. 55-60.

15. Weyhe, D., P. Hoffmann, O. Belyaev, K. Mros, C. Muller, W. Uhl, and F. Schmitz, *The role of TGF-b1 as a determinant of foreign body reaction to alloplastic materials in rat fibroblast cultures: comparison of different commercially available polypropylene meshes for hernia repair.* Regulatory Peptides, 2007. **138**(1): p. 10-14.

16. Greca, F.H., J.B. De Paula, and M. Binnebösel, *Then influence of differing pore size on the biocompatibility of two polypropylene mehses in the repair of abdominal defects. Experiment study in dogs.* Hernia, 2000(5): p. 59-64.

17. Jansen, P.L., P.R. Mertens, U. Klinge, and V. Schumpelick, *The biology of hernia formation.* Surgery, 2004. **136**(1): p. 1-4.

18. Bellon, J., A. Bajo, N. Ga-Honduvilla, M. Gimeno, G. Pascual, A. Guerrero, and J. Bujan, *Fibroblasts from he transversali fascia of young petients with direct inguinal hernias show constritutive MMP-2 overespression.* Annals of Surgery, 2001. **233**: p. 287-291.

19. Zheng, H., R. Kasperk, B. RS, V. Schumpelick, U. Klinge, and B. Klosterhalfen, *Recurrent inguinal hernia: disease of the collagen matrix?* World Journal of Surgery, 2002. **26**: p. 401-408.

20. Friedman, D., C. Boyd, P. Norton, R. Greco, A. Boyarsi, J. Mackenzie, and S. Deak, *Increased in Type III collagen expression in protein synthesis in patients with inguinal hernias.* Annals Surgery, 1993. **218**: p. 754-760.

21. Benjamin, M. and B. Hillen, *Mechanical influences on cells, tissue and organs - ' mechanical morphogenesis'.* European Journal of Morphology, 2003. **41**(1): p. 3-7.

22. Woods, B. and L. Naumayer, *Open Repair of Inguinal Hernia: An Evidence-Based Review.* Surgical Clinics of North America, 2008. **88**(1): p. 139-155.

23. Matthews, R.D. and L. Neumayer, *Inguinal Hernia in the 21st Century: An Evidence-Based Review.* Current Problems in Surgery, 2008. **45**(4): p. 261-312.

24. van Veen, R., A. Wijsmuller, W. Vrijland, W. Hop, and J. Lange, *Long-term follow-up of a randomized clinical trial of non-mesh versus mesh repair of primary inguinal hernia.* British Journal of Surgery, 2007. **94**(6): p. 506-510.

25. Mokete, M. and J. Earnshaw, *Evolution of an inguinal hernia surgery practice.* Postgraduate Medical Journal, 2001. **77**: p. 188-190.

26. Anderson, J.M., A. Rodriguez, and D.T. Chang, *Foreign body reaction to biomaterials.* Seminar in Immunology, 2008. **20**: p. 86-100.

27. Earle, D.B. and L.A. Mark, *Prosthetic Material in Inguinal Hernia Repair: How Do I Choose?* Surgical Clinics of North America, 2008. **88**: p. 179-201.

28. Klosterhalfen, B., B. Hermanns, R. Rosch, and K. Junge, *Biological Response to Mesh.* European Surgical Research, 2003. **35**(1): p. 16-20.

29. Massaron, S., S. Bona, U. Fumagalli, F. Battafarano, U. Elmore, and R. Rosati, *Analysis of post-surgical pain after inguinal hernia repair: a pospective study of 1,440 operations.* Hernia, 2007. **11**: p. 517-525.

30. Grant, A., N. Scott, and P. O' Dwyer, *Five-year follow-up of a randomized trial to assess pain and numbness after laparoscopic or open repair of groin hernia.* British Journal of Surgery, 2004. **91**: p. 1570-1574.

31. Nienhuijs, S., E. Staal, L. Strobbe, C. Rosman, H. Groenewoud, and R. Bleichrodt, *Chronic pain after mesh repair of inguinal hernia: a systematic review.* American Journal of Surgery, 2007. **194**: p. 394-400.

32. Klosterhalfen, B., U. Klinge, U. Henze, R. Bhardwaj, C. J., and V. Schumpelic, *Morphologic correlation of functional abdominal wall mechanics after mesh implantation.* Langenbecks Archiv für Chirurgie, 1997. **382**(2): p. 87-94.

33. Welty, G., U. Klinge, and B. Klosterhalfen, *Functional impairment and complaints following incisional hernia repair with different polypropylene meshes.* Hernia, 2001. **5**: p. 142.

34. Badylak, S., K. Kokini, B. Tullius, A. Simmons-Byrd, and R. Morff, *Morphologic Study of Small Intestinal Submucosa as a Body Wall Repair Device.* Journal of Surgical Research, 2002. **103**(2): p. 190-202.

35. Earle, D.B. and L.A. Mark, *Prosthetic Materials in Inguinal Hernia Repair: How Do I Choose.* Surgical Clinics of North America, 2008. **88**: p. 179-201.

36. Bellows, C., A. Alder, and W. Helton, *Abdominla wall reconstruction using biological tissue grafts: present status and future opportunites.* Expert Review of Medical Devices, 2006. **3**(5): p. 657-675.

37. Gonzalez, R., K. Fugate, D. McClusky III, M. Ritter, A. Lederman, D. Dillehay, D. Smith, and B.J. Ramshaw, *Relationship Between Tissue Ingrowth and Mesh Contraction.* World Journal of Surgery, 2005. **29**: p. 1038-1043.

38. Ambrosiani, N., J. Harb, and A. Gavelli, *Failure of the treatment of eventration and hernias with the PTFE plates (111 cases).* Ann Chir, 1994. **48**(10): p. 917-920.

39. Sikkink, C., T. Vries de Reilingh, and A. Malyar, *Adhesion formation and reherniation differ between meshes used for abdominal wall reconstruction.* Hernia, 2006. **10**(3): p. 218-222.

40. Bachman, S. and B. Ramshaw, *Prosthetic Materials in Ventral Hernia Repair: How Do I Choose?* Surgical Clinics of North America, 2008. **88**: p. 101-112.

41. Karamuk, E., J. Mayer, and G. Raeber, *Tissue engineered composite of a woven fabric scaffold with tendon cells, response on mechanical simulation in vitro.* Composites Science and Technology, 2004. **64**(6): p. 885-891.

42. de Haan, J., *Structure-property relations in plain weft-knitted fabric reinforced composites (KFRCs) preparing for loading bearing implants: experimental study and beam model approach.*, in *Department of Materials*. 1999, ETH Zurich.

43. Klinge, U., B. Klosterhalfen, M. Muller, M. Anurov, A. Ottigner, and V. Schumpelick, *Influence of polyclactin-coating on functional and morphological parameters of polypropylene-mesh modificaiton for abdominla wall repair.* Biomaterials, 1999. **20**: p. 613-623.

44. Klosterhalfen, B., U. Klinge, and V. Schumpelick, *Functional and morphological evaluation of different polypropylene-mesh modifications for abdominal wall repair.* Biomaterials, 1998. **19**: p. 2235-2246.

45. Klosterhalfen, B., U. Klinge, B. Hermanns, and V. Schumpelick, *Pathology of traditional surgical nets for hernia repair after long-term implantation in humans.* Chirurg, 2000. **71**: p. 43-51.

46. Schumpelick, V., U. Klinge, G. Welty, and B. Klosterhalfen, *Meshes within the abdominla well.* Chirurg, 1999. **70**: p. 876-887.

47. Meaney, D.F., *Mechanical properties of implantable biomaterials.* Clinics in podiatric medicine and surgery, 1995. **12**(3): p. 363-384.

48. Bruinink, A., G. Siragusano, G. Ettel, T. Brandsberg, F. Brandsberg, M. Petitmermet, M. Muller, E. Mayer, and E. Wintermantel, *The stiffness of bone marrow cell-knit compoistes is increased during mechanical load.* Biomaterials, 2001. **22**: p. 3169-3178.

49. Klinge, U., B. Klosterhalfen, J. Conze, W. Limberg, B. Obolenski, A.P. Ottinger, and V. Schumpelick, *Modified mesh for hernia repair that is adapted to the physiology of the abdominal wall.* The European Journal Of Surgery = Acta Chirurgica, 1998. **164**(12): p. 951-960.

50. Kirkpatrick, C., M. Otto, T. Van Kooten, J. Kriegsmann, and B. F, *Endothelial cell culture as a tool in biomaterial research.* Journal of Materials Science: Materials in Medicine, 1999. **10**: p. 589-594.

51. Kirkpatrick, C., M. Otto, T. Van Kooten, V. Krump, J. Kriegsmann, and F. Bittinger, *Endothelial cell culture as a tool in biomaterial research.* Journal of Materials Science: Materials in Medicine, 1999. **10**(10/11): p. 589-594.

52. Stadelmann, W., A. Digenis, and T. GR, *Physiology and healing dynamics of chronic cutaneous wounds.* American Journal of Surgery, 1998. **176**: p. 26-38S.

53. Morrison, C., R. Macnair, C. MacDonald, A. Wykman, I. Goldie, and M.H. Grant, *In vitro biocompatibility testing of polymers for orthopaedic implants using cultured fibroblasts and osteoblasts.* Biomaterials, 1995. **16**(13): p. 987-992.

54. Wiegand, C. and U.C. Hipler, *Evaluation of biocompatibility and cytotoxicity using keratinocyte and fibroblast cultures.* Skin Pharmacology And Physiology, 2009. **22**(2): p. 74-82.

55. Langer, C., P. Schwartz, H. Mohammadi, B. Kulle, A. Schaper, L. Fuzesi, and H. Becker, *In-vitro study of the cellular response of human fibroblasts cultured on alloplastic hernia meshes. Inflence of mesh material and structure.* Chirurg, 2005(76): p. 876-885.

56. Menard, K.P., *Dynamic Mechanical Analysis: A Practical Introduction*. 1999: CRC Press LLC.

57. Amid, P.K., *Classifcation of biomaterials and their related complications in abdominal wall hernia surgery.* Hernia, 1997(1): p. 15-21.

58. Bethge, T., M. Duchrow, U. Windhovel, and R. Broll, *Growth inhibition of human fibroblasts by resterilized polypropylene meshes.* Chirurgisches Forum fuer Experimentelle und Kinische Forschung, 2002(173-175).

59. Bellón, J.M., J. Buján, L. Contreras, and A. Hernando, *Integration of biomaterials implanted into abdominal wall: process of scar formation and macrophage response.* Biomaterials, 1995. **16**(5): p. 381-387.

60. Hallab, N.J., K.J. Bundy, K. O' Connor, R.L. Moses, and J.J. Jacobs, *Evaluation of Metallic and Polymeric Biomaterial Surface Energy and Surface Roughness Characteristics for Directed Cell Adhesion.* Tissue Enginnering, 2001. **7**(1): p. 55-71.

61. Dumitriu, S., ed. *Polymeric biomaterials*. Textile-Based Biomaterials for Surgical Applicaitons, ed. C.C. Chu. 2002, Marcel Dekker, Inc. 491-544.

62. Wilkins, K.M., G.P. Martin, G.W. Hanlon, and C. Marriott, *The influence of critical surface tension and microrugosity on the adhesion of bacteria to polymer monofilaments.* International Journal of Pharmaceutics, 1989. **57**: p. 1-7.

63. Ratner, B.D., A.S. Hoffman, F.J. Schoen, and J.E. Lemons, *Biomaterials Science: An Introduction to Materials in Medicine, 2nd Edition*. 2004: Elsevier Academic Press.

64. Klinge, U., B. Klosterhalfen, V. Birkenhauer, K. Junge, J. Conze, and V. Schumpelick, *Impact of Polymer Pore Size on the Interface Scar Formation in a Rat Model.* Journal of Surgical Research, 2002. **103**(2): p. 208-214.

65. Khan, L.R., S. Liong, A.C.d. Beaux, S. Kumar, and S.J. Nixon, *Lightweigh mesh improve functional outcome in laparoscopic totally extra-peritoneal inguinal hernia repair.* Hernia, 2010. **14**: p. 39-45.

66. Lam, K.H., J.M. Schakenraad, H. Groen, H. Esselbrugge, P.J. Dijkstra, J. Feijen, and P. Nieuwenhuis, *The influence of surface morphology and wettability on the inflammatory response against poly(L-lactic acid): A semi-quantitative study with monoclonal antibodies.* Journal of Biomedical Materials Research, 1995. **29**(8): p. 929-942.

67. Iwasaki, Y., S.-i. Sawada, K. Ishihara, G. Khang, and H.B. Lee, *Reduction of surface-induced inflammatory reaction on PLGA/MPC polymer blend.* Biomaterials, 2002. **23**(18): p. 3897-3903.

68. Marois, Y., R. Cadi, J. Gourdon, N. Fatouraee, M.W. King, Z. Zhang, and R. Guidoin, *Biostability, inflammatory response, and healing characteristics of a fluoropassivated polyester-knit mesh in the repair of experimental abdominal hernias.* Artificial Organs, 2000. **24**(7): p. 533-543.

69. Rosch, R., K. Junge, A. Schachtrupp, U. Klinge, B. Klosterhalfen, and V. Schumpelick, *Mesh Implants in Hernia Repair.* European Surgical Research, 2003. **35**(3): p. 161-166.

APPENDICES

1. Optical density of formazan solution to determine cell proliferation of NRK-49F cells after contacting with different prosthetic meshes.

a. Data

Sample	**PP403**	**PP404**	**PP601**	**PET**	**PTFE**	**CON.**
OD, × 10^{-3}	0.514	0.517	0.539	0.48	0.433	0.468
	0.517	0.512	0.537	0.481	0.428	0.470
	0.517	0.512	0.525	0.473	0.428	0.468
	0.514	0.512	0.534	0.478	0.432	0.468
	0.521	0.517	0.538	0.496	0.423	0.470
Average	0.517	0.514	0.536	0.482	0.429	0.469
SD	0.002881	0.002739	0.005683	0.00862	0.003962	0.001095

b. Statistical analysis

One-way ANOVA: OD versus mesh

Note: Level
1 PP403 mesh
2 PP404 mesh
3 PP601 mesh
4 PET mesh
5 PTFE mesh
6 Control

```
Source  DF         SS         MS       F      P
mesh     5  0.0376747  0.0075349  324.55  0.000
Error   24  0.0005572  0.0000232
Total   29  0.0382319

S = 0.004818   R-Sq = 98.54%   R-Sq(adj) = 98.24%


                           Individual 95% CIs For Mean Based on Pooled StDev
Level  N     Mean    StDev  ---------+---------+---------+---------+
1      5  0.51660  0.00288                                (*-)
2      5  0.51400  0.00274                               (*-)
3      5  0.53460  0.00568                                      (*-)
4      5  0.48160  0.00862                    (-*)
5      5  0.42880  0.00396  (-*)
6      5  0.46880  0.00110               (*-)
                           ---------+---------+---------+---------+
```

```
                                0.450     0.480     0.510     0.540

Fisher 95% Individual Confidence Intervals
All Pairwise Comparisons among Levels of mesh

Simultaneous confidence level = 66.17%


mesh = 1 subtracted from:

mesh     Lower    Center     Upper  ---------+---------+---------+---------+
2     -0.00889  -0.00260   0.00369                   (*)
3      0.01171   0.01800   0.02429                      (*)
4     -0.04129  -0.03500  -0.02871             (*)
5     -0.09409  -0.08780  -0.08151     (*)
6     -0.05409  -0.04780  -0.04151            (*)
                                    ---------+---------+---------+---------+
                                          -0.060     0.000     0.060     0.120


mesh = 2 subtracted from:

mesh     Lower    Center     Upper  ---------+---------+---------+---------+
3      0.01431   0.02060   0.02689                      (*)
4     -0.03869  -0.03240  -0.02611              (*)
5     -0.09149  -0.08520  -0.07891      (*)
6     -0.05149  -0.04520  -0.03891            (*-)
                                    ---------+---------+---------+---------+
                                          -0.060     0.000     0.060     0.120


mesh = 3 subtracted from:

mesh     Lower    Center     Upper  ---------+---------+---------+---------+
4     -0.05929  -0.05300  -0.04671          (*)
5     -0.11209  -0.10580  -0.09951  (*)
6     -0.07209  -0.06580  -0.05951         (*)
                                    ---------+---------+---------+---------+
                                          -0.060     0.000     0.060     0.120


mesh = 4 subtracted from:

mesh     Lower    Center     Upper  ---------+---------+---------+---------+
5     -0.05909  -0.05280  -0.04651          (*)
6     -0.01909  -0.01280  -0.00651                 (*)
                                    ---------+---------+---------+---------+
                                          -0.060     0.000     0.060     0.120


mesh = 5 subtracted from:

mesh    Lower   Center    Upper  ---------+---------+---------+---------+
6     0.03371  0.04000  0.04629                        (*)
                                ---------+---------+---------+---------+
                                      -0.060     0.000     0.060     0.120
```

2. Elastic modulus of vital/avital composite mesh compared with its control (without cells)

a. Data

Elastic modulus, MPa	1	2	3	**Average**	**SD**
PP403 control	4.22	5.11	4.91	4.75	0.469761
PP403 composite	5.23	5.91	5.96	5.70	0.407799
PP404 control	3.97	3.21	3.77	3.65	0.393954
PP404 composite	4.10	3.98	4.73	4.27	0.402865
PP601 control	9.51	9.44	8.17	9.04	0.754255
PP601 composite	13.7	12.9	13.92	13.51	0.546168
PET control	8.25	7.33	8.21	7.93	0.520000
PET composite	14.6	15.07	15.87	15.17	0.660328
PTFE control	2.72	3.71	3.95	3.46	0.651997
PTFE composite	4.54	4.15	3.79	4.16	0.375100

b. Statistical analysis

1) PP403 mesh

```
Sample  N   Mean  StDev  SE Mean
1       3  4.745  0.470     0.27
2       3  5.700  0.408     0.24


Difference = mu (1) - mu (2)
Estimate for difference:  -0.955
95% CI for difference:  (-2.098, 0.188)
T-Test of difference = 0 (vs not =): T-Value = -2.66  P-Value = 0.076  DF = 3
```

2) PP404 mesh

```
Sample  N   Mean  StDev  SE Mean
1       3  3.650  0.394     0.23
2       3  4.270  0.403     0.23


Difference = mu (1) - mu (2)
Estimate for difference:  -0.620
95% CI for difference:  (-1.655, 0.415)
T-Test of difference = 0 (vs not =): T-Value = -1.91  P-Value = 0.153  DF = 3
```

3) PP601 mesh

```
Sample  N    Mean  StDev  SE Mean
1       3   9.040  0.754     0.44
2       3  13.510  0.546     0.32


Difference = mu (1) - mu (2)
Estimate for difference:  -4.470
95% CI for difference:  (-6.181, -2.759)
T-Test of difference = 0 (vs not =): T-Value = -8.31  P-Value = 0.004  DF = 3
```

4) PET mesh

```
Sample  N    Mean  StDev  SE Mean
1       3   7.930  0.520     0.30
2       3  15.167  0.660     0.38


Difference = mu (1) - mu (2)
Estimate for difference:  -7.237
95% CI for difference:  (-8.781, -5.692)
T-Test of difference = 0 (vs not =): T-Value = -14.91  P-Value = 0.001  DF = 3
```

5) PTFE mesh

```
Sample  N   Mean  StDev  SE Mean
1       3  3.460  0.652     0.38
2       3  4.160  0.375     0.22


Difference = mu (1) - mu (2)
Estimate for difference:  -0.700
95% CI for difference:  (-2.082, 0.682)
T-Test of difference = 0 (vs not =): T-Value = -1.61  P-Value = 0.205  DF = 3
```

3. Ultimate strength of vital/avital composite mesh compared with its control (without cells)

a. Data

Ultimate strength, kPa	1	2	3	**Average**	**SD**
PP403 control	53.37	54.09	59.34	55.60	3.258880
PP403 composite	70.23	67.01	72.01	69.75	2.534324
PP404 control	50.99	51.02	57.38	53.13	3.680639
PP404 composite	67.09	69.21	63.71	66.67	2.773950
PP601 control	153.12	155.10	157.53	155.25	2.208823
PP601 composite	162.39	163.09	168.23	164.57	3.188918
PET control	140.90	130.57	128.43	133.3	6.668201
PET composite	171.40	173.60	186.63	177.21	8.231786
PTFE control	31.56	31.67	28.35	30.53	1.885851
PTFE composite	18.23	16.84	18.12	17.73	0.772722

b. Statistical analysis

1) PP403 mesh

```
Sample  N   Mean  StDev  SE Mean
1       3  55.60   3.26      1.9
2       3  69.75   2.53      1.5


Difference = mu (1) - mu (2)
Estimate for difference:  -14.15
95% CI for difference:  (-21.74, -6.56)
T-Test of difference = 0 (vs not =): T-Value = -5.94  P-Value = 0.010  DF = 3
```

2) PP404 mesh

Sample	N	Mean	StDev	SE Mean
1	3	53.13	3.68	2.1
2	3	66.67	2.77	1.6

Difference = mu (1) - mu (2)
Estimate for difference: -13.54
95% CI for difference: (-22.01, -5.07)
T-Test of difference = 0 (vs not =): T-Value = -5.09 P-Value = 0.015 DF = 3

3) PP601 mesh

Sample	N	Mean	StDev	SE Mean
1	3	155.25	2.21	1.3
2	3	164.57	3.19	1.8

Difference = mu (1) - mu (2)
Estimate for difference: -9.32
95% CI for difference: (-16.45, -2.19)
T-Test of difference = 0 (vs not =): T-Value = -4.16 P-Value = 0.025 DF = 3

4) PET mesh

Sample	N	Mean	StDev	SE Mean
1	3	133.30	6.67	3.8
2	3	177.21	8.23	4.8

Difference = mu (1) - mu (2)
Estimate for difference: -43.91
95% CI for difference: (-63.37, -24.45)
T-Test of difference = 0 (vs not =): T-Value = -7.18 P-Value = 0.006 DF = 3

5) PTFE mesh

1	3	30.53	1.89	1.1
2	3	17.730	0.772	0.45

Difference = mu (1) - mu (2)
Estimate for difference: 12.80
95% CI for difference: (7.73, 17.86)
T-Test of difference = 0 (vs not =): T-Value = 10.88 P-Value = 0.008 DF = 2

4. Storage modulus of vital/avital composite mesh and its control (without cells)

PP403 vital/avital composite mesh

Time	1	2	3	**Storage modulus, Pa**		**Percent change, %**	
				average	sd	average	sd
0	9.29E+05	9.530E+05	1.07E+06	9.85E+05	7.72E+04	0	0
180	9.15E+05	9.71E+05	1.07E+06	9.85E+05	7.74E+04	-0.01914	0.786085
240	1.34E+06	1.39E+06	1.43E+06	1.39E+06	4.60E+04	40.78526	0.331973
420	9.90E+05	1.05E+06	1.10E+06	1.05E+06	5.42E+04	6.1068	0.518834
480	1.39E+06	1.45E+06	1.47E+06	1.44E+06	4.52E+04	45.84913	0.314752
660	1.08E+06	1.17E+06	1.08E+06	1.11E+06	5.21E+04	12.7395	0.469567

PP404 control mesh

Time	**Storage modulus, Pa**	**Percent change, %**
0	916203.4	0
180	9.154E+05	-0.08475
240	1.004E+06	9.573919
420	8.716E+05	-4.86806
480	1.047E+06	14.32614
660	8.398E+05	-8.3359

PP404 vital/avital composite mesh

Time	1	2	3	**Storage modulus, Pa**		**Percent change, %**	
				average	sd	average	sd
0	7.34E+05	6.00E+05	6.50E+05	6.61E+05	6.78E+04	0	0
180	7.37E+05	5.99E+05	6.24E+05	6.53E+05	7.38E+04	-1.20957	1.129238
240	8.78E+05	7.56E+05	7.67E+05	8.00E+05	6.75E+04	21.03677	0.842726
420	7.46E+05	6.35E+05	6.54E+05	6.78E+05	5.94E+04	2.514150	0.876234
480	8.90E+05	7.48E+05	8.09E+05	8.160E+05	7.10E+04	23.28054	0.870233
660	7.67E+05	6.45E+05	6.52E+05	6.88E+05	6.88E+04	4.039280	0.999970

PP404 control mesh

Time	**Storage modulus, Pa**	**Percent change, %**
0	628901	0
180	619529.6	-1.49012
240	711641.3	13.15633
420	611430.9	-2.77787
480	700984.1	11.46176
660	604818.8	-3.82924

PP601 vital/avital composite mesh

Time	1	2	3	**Storage modulus, Pa**		**Percent change, %**	
				average	sd	average	sd
0	1.35E+06	1.47E+06	1.39E+06	1.40E+06	6.02E+04	0	0
180	1.34E+06	1.46E+06	1.38E+06	1.39E+06	6.08E+04	-0.7646	0.65188
240	1.70E+06	1.79E+06	1.68E+06	1.72E+06	6.06E+04	22.8115	0.65824
420	1.50E+06	1.61E+06	1.56E+06	1.56E+06	5.45E+04	11.0391	0.75032
480	1.73E+06	1.74E+06	1.86E+06	1.78E+06	6.89E+04	26.7440	0.682723
660	1.61E+06	1.62E+06	1.71E+06	1.65E+06	5.29E+04	17.3119	0.62178

3b) PP601 control mesh

Time	**Storage modulus, Pa**	**Percent change, %**
0	977261.3	0
180	976628.5	-0.06475
240	960859.5	-1.67834
420	939460.2	-3.86806
480	917170.3	-6.14892
660	905570.4	-7.33590

PET vital/avital composite mesh

Time	1	2	3	**Storage modulus, Pa**		**Percent change**	
				average	sd	average	sd
0	1.68E+06	1.63E+06	1.57E+06	1.63E+06	5.83E+04	0	0
180	1.68E+06	1.62E+06	1.54E+06	1.61E+06	6.82E+04	-0.81202	0.422605
240	1.80E+06	1.74E+06	1.69E+06	1.75E+06	5.36E+04	7.27067	0.306947
420	1.62E+06	1.54E+06	1.50E+06	1.55E+06	6.16E+04	-4.56538	0.396775
480	1.72E+06	1.71E+06	1.61E+06	1.68E+06	6.25E+04	3.31262	0.371971
660	1.62E+06	1.54E+06	1.52E+06	1.56E+06	5.38E+04	-4.08530	0.345086

PET control mesh

Time	**Storage modulus, Pa**	**Percent change, %**
0	864630.521	0
180	848963.243	-1.81202
240	831570.422	-3.82361
420	816510.547	-5.56538
480	796297.041	-7.90320
660	788739.306	-8.77730